Research Article
Geochemistry, Geophysics, Geosystems
DOI 10.1002/2013GC005133

Active alkaline traps to determine acidic-gas ratios in volcanic plumes: sampling techniques and analytical methods

J. Wittmer, N. Bobrowski, M. Liotta, G. Giuffrida, S. Calabrese and U.Platt

Authors

Julian Wittmer,

A: Atmospheric Chemistry Research Laboratory, University of Bayreuth, Bayreuth, Germany.

B: Institute of Environmental Physics, University of Heidelberg, Heidelberg, Germany.

Nicole Bobrowski and Ulrich Platt, Institute of Environmental Physics, University of Heidelberg, Heidelberg, Germany.

Marcello Liotta,

A: Department DiSTABiF, Second University of Naples, Caserta, Italy.

B: Istituto Nazionale di Geofisica e Vulcanologia, Palermo, Italy.

Giovanni Giuffrida, Istituto Nazionale di Geofisica e Vulcanologia, Palermo, Italy.

Sergio Calabrese, Department DiSTeM, University of Palermo, Palermo, Italy.

Corresponding author: J. Wittmer, Atmospheric Chemistry Research Laboratory, University of Bayreuth, 95448 Bayreuth, Germany. (Julian.Wittmer@uni-bayreuth.de)

This article has been accepted for publication and undergone full peer review but has not been through the copyediting, typesetting, pagination and proofreading process which may lead to differences between this version and the Version of Record. Please cite this article as doi: 10.1002/2013GC005133

Received: Nov 06, 2013; Revised: Feb 11, 2014; Accepted: Jun 02, 2014

Abstract

In-situ measurements have been the basis for monitoring volcanic gas emissions for many years and - being complemented by remote sensing techniques - still play an important role to date. Concerning in-situ techniques for sampling a dilute plume, an increase in accuracy and a reduction of detection limits are still necessary for most gases (e.g. CO_2, SO_2, HCl, HF, HBr, HI). In this work the Raschig-Tube technique (RT) is modified and utilized for application on volcanic plumes. The theoretical and experimental absorption properties of the RT and the Drechsel bottle (DB) set-ups are characterized and both are applied simultaneously to the well-established Filter packs technique (FP) in the field (on Stromboli Island and Mount Etna). The comparison points out that FPs are the most practical to apply but the results are error-prone compared to RT and DB, whereas the RT results in up to 13-times higher analyte concentrations than the DB in the same sampling time. An optimization of the analytical procedure, including sample pre-treatment and analysis by titration, Ion Chromatography, and Inductively Coupled Plasma Mass Spectrometry, led to a comprehensive data set covering a wide range of compounds. In particular, less abundant species were quantified more accurately and iodine was detected for the first time in Stromboli's plume. Simultaneously applying Multi-Axis Differential Optical Absorption Spectroscopy (MAX-DOAS) the chemical transformation of emitted bromide into bromine monoxide (BrO) from Stromboli and Etna was determined to 3-6% and 7%, respectively, within less than 5 minutes after the gas release from the active vents.

1. Introduction and background

Gases released from magma provide useful information on the chemico-physical features of the magmatic system [e.g. *Jagger,* 1940; *Sparks*, 2003]. They have been subject of several studies based on soil degassing measurements [e.g. *Chiodini et al.*, 1996], direct sampling of fumaroles [e.g. *Giggenbach and Matsuo*, 1991; *Symonds et al.,* 1994], and in-situ as well as remote sensing measurements of volcanic plumes [e.g. *Symonds et al.,* 1994; *McGonigle and Oppenheimer,* 2003].

Volcanic plumes are a mixture of gas, and liquid and solid particles. The most abundant gases are H_2O and CO_2 followed in descending abundance by SO_2, H_2S, HCl, HF, HBr, and minor amounts of H_2, CO, OCS, Ar, NH_4, CH_4, N_2 and He, and many more [e.g. *Symonds et al.,* 1994]. Studying volcanic gases is motivated on the one hand because of their effects on atmosphere and climate and on the other hand because they indicate sub-surface magmatic processes. Open vent degassing is one of the most direct manifestations of magmatic degassing. In-situ sampling techniques that are as close as possible to the emission source are the most suitable tools to provide as much information as possible on the primary emitted volcanic gases. The thus gained molar composition can be used to infer the initial volcanic gas composition considering the effect on gas chemistry of secondary processes due to cooling, gas-gas and gas-rock interactions. Some volcanic gases are rapidly transformed due to the transition from reducing to oxidizing conditions as soon as volcanic volatiles start to mix with the surrounding atmosphere, which results in a very fast change of the composition of the gas-particulate mixture. HBr, for instance, can take part in fast reactions involving ozone from the surrounding atmosphere [e.g. *Bobrowski et al.*, 2003; *Oppenheimer et al.,* 2006; *Bobrowski et al.*, 2007; *von Glasow et al.*, 2009]. Combining in-situ sampling with remote sensing measurements helps to observe the evolving chemistry by the mixing of volcanic and atmospheric gases and particles [*Oppenheimer et al.,* 2006].

Active in-situ sampling techniques for plume gases are usually based on open system samplers where a pump allows a large volume of volcanic gas to pass through a medium (e.g. filter, impregnated filter, alkaline, neutral, acidic solutions or combination of them in a row), which is able to trap volcanogenic compounds for later analysis [e.g. *Roberts and Mckee,* 1959*; Finnegan et al.,* 1989*; Aiuppa* 2009*; Liotta et al.,* 2012]. Each of the sampling techniques has individual strengths and weaknesses come along that influences the results. Moreover, the quality of the results is also affected by the sample preparation and analyzing techniques. The main aim of this paper is (i) to describe and characterize the Raschig-Tube method in terms of volcanic plume sampling close to the active degassing vents, (ii) investigate and compare the efficiency of existing active alkaline traps for volcanic plume sampling and their connected analyzing processes, and (iii) to determine a

state of the art for the investigation of acidic gases in volcanic plumes with reliable results. This is done with a particular focus on halogen species.

The principle challenges with in-situ measurements include difficult access to the emissions, and dilution of plume constituents with atmospheric gases in terms of the evolving chemistry and the lower volcanic gas concentrations with increasing distance to the magma surface. For instance at Stromboli volcano, only a few studies on plume gas composition obtained by direct sampling techniques (Filter-packs and diffusive tubes) are available, which were obtained by direct sampling techniques [e.g.; *Allard et al.*, 2000; *Aiuppa and Federico*, 2004]. In the last decade, due to technical evolutions, most researchers concentrated on remote sensing techniques like Open-Path Fourier Transform Infrared (OP-FTIR) spectroscopy [*Burton et al*., 2007; *La Spina et al*., 2013], SO_2 imaging camera [*Mori and Burton*, 2009] or Differential Optical Absorption Spectroscopy (DOAS) [e.g. *Burton et al.*, 2009; *Bobrowski and Platt*, 2007] to investigate Stromboli's plume.

In this work some of the measurements were accompanied by the established remote sensing method – MAX-DOAS technique [*Platt and Stutz,* 2008]. Bromine monoxide (BrO) and SO_2 were detected with a MAX-DOAS instrument downwind. The resulting BrO/SO_2 ratios are compared to Br/S ratios obtained by direct sampling (see section 5.4). Whereas in-situ techniques are sensitive to the main initial bromine compound HBr, the detection of HBr is still challenging for remote sensing techniques. In recent years the bromine chemistry within the plume and the rate of BrO formation was investigated by model and field studies [e.g. *von Glasow*, 2010; *Roberts et al.*, 2009; *Bobrowski and Platt*, 2007]. Although, in-situ and remote sensing techniques complement each other simultaneous measurements are still rare.

In addition, so far volcanic iodine chemistry has not been given much consideration due to difficulties in detection. Estimates of the global volcanic iodine flux range from 0.11 kt yr^{-1} [*Aiuppa et al.*, 2005a] to about 0.2 – 7.7 kt yr^{-1} [*Snyder and Fehn*, 2002] or roughly 1 % of the bromine flux. Probably I is dominantly released as hydrogen iodide (HI) [e.g. *Honda*, 1970] and could eventually form the reactive halogen species iodine oxide (IO). However, iodine oxides have not been detected yet. Volcanic iodine in the gas phase of a plume was only investigated a few times in the past after the absorption of iodine compounds on a filter [e.g. *Aiuppa et al.*, 2005a; *Witt et al.*, 2008] and detection by ICP-MS. Most studies focus on the detection of iodine in fumaroles [*Honda*, 1966, 1970; *Tedesco and Toutain*, 1991] or in volcanic fluids, where the origin of iodine is localized in the deep parts of the subduction zone and the overlying crust [*Snyder and Fehn*, 2002].

2. Methods

Active alkaline traps, as used in this work, consist of an alkaline solution that is exposed to the sample media by pumping the plume-atmosphere mixture through it. The alkaline solution captures acidic species due to the acid-base reactions. Sampling was performed with a GilAir Plus pump (Sensidyne) that guarantees a constant flow rate (automatic adjustment depending on the backpressure of the instrument) and allows to register the sampled air volume with a low uncertainty (± 5% given by the manufacturer). The various alkaline traps were applied simultaneously in the field in order to compare the sampling characteristics and the resulting molar ratios. No particle filter was used in front of the instruments to be able to determine the total molar ratio including all volcanogenic products generating from the gas phase and to avoid interactions between volcanic aerosol, potentially condensing water, and acidic gases accumulating on the particle filter. Anyway, the contribution of particles to the total molar amount of trapped species is hard to estimate e.g. depending on the location of the volcano, the state of activity and anthropogenic influences (see section 5.1.2). Plume chemistry, including composition and plume age, can be affected by meteorological parameters; therefore meteorological data were recorded during the sampling by a portable weather station (Kestrel) and are presented in Table 1.

The samples are pretreated and analyzed for the composition by Ion Chromatography (IC) and Inductively Coupled Plasma mass spectrometry (ICP-MS) to quantify the elements of interest. Concerning the applied alkaline traps and the associated analysis each parameter was optimized as good as possible (reaction surface, flux, sample pretreatment – see 2.2, etc.) in order to obtain elemental concentrations that meet analytical detection limit in a as short as possible sampling time period to reduce the sampling time and hazardous risks.

2.1. Sampling techniques

2.1.1. Filter-pack

The active gas filtration method, so called “Filter-pack” (FP), basically consists of a set of several impact filters impregnated with a suitable alkaline material, which are mounted in series (i.e. the sample air sequentially flows through all filters) into a sealed filter holder system (sampling cassette), which is connected to an air sampling pump [e.g. *Huygen,* 1962; *Finnegan et al.*, 1989; *Aiuppa* 2009 and reference therein]. Many variations were developed in the past applying different kinds of basic solutions (e.g. NaOH, LiOH, KOH, $NaHCO_3$) to impregnate different kinds of filters (e.g. cellulose, nylon or Teflon) [e.g. *Stoiber*, 1986; *Witter and Delmelle*, 2004; *Mather and Pyle*, 2008], using glycerol to improve the absorption efficiency [*Huygen*, 1962, 1963], or mounting a particle filter on the top in order to minimize uptake of airborne aerosols and ash particles [*Finnegan et al.*, 1989]. Moreover, Filter-packs (non-impregnated) have also been used to estimate

the flux of trace metals from volcanoes [*Calabrese et al.*, 2011]. Despite the improvements, the efficiency of filter packs can be reduced since they can reach saturation relatively fast [*Mioduszewski and Kress*, 2008]. As a general rule, when the last filter of the pack contains non-negligible amounts (>10%) of the total trapped species, results should be discarded. *Mioduszewski and Kress* [2008] investigated the filter pack method by sampling an artificial fumarole and found that extreme caution must be paid to maintain strong under-saturation with respect to acid gases in order to avoid the underestimation of S/Cl and S/F ratios. Because of their easy applicability, filter packs are in widespread use and extensive data sets have been accumulated using this approach [e.g. *Aiuppa* 2009].

The number of filters placed in series determines the parameters for application in the field (flow rate, sampling time etc.). In this work three filters (filter papers 541 hardened ashless, 47 mm diameter cat n° 1441 047 from Whatman) in a pack were used (named A - first, B - middle, C – last respectively), impregnated with a 1 M $NaHCO_3$ solution with 10% glycerol.

2.1.2. Drechsel bottle

Sampling systems based on gas washing bottles named after Edmund Drechsel (Drechsel Bottle's, DB) consist of glassware which uses a fritted glass piece (frit) fused to the tip of a gas-inlet tube reaching the bottom of the device. In operation the DB is filled with an absorber solution (in this work 100 ml of 1 Molar sodium hydroxide solution – NaOH) and air is drawn through the device, which causes small bubbles to emerge from the frit. During the rise time of the bubbles through the liquid a diffusive transport of airborne compounds into the solution takes place.

DBs and comparable types of washing bottles have a long history in atmospheric science [e.g. *Roberts and Mckee*, 1959; *Gage*, 1960] but are less common for volcanic gas sampling due to the fragileness of the components and the intricate set-up for such an environment. Recently *Liotta et al.* [2012] and *Rizzo et al.* [2013] successfully used a DB to trap volcanogenic gases from the plume of Mt. Etna in order to determine the isotopic composition of sulfur and chlorine, respectively. In this work a DB set up according to *Liotta et al.* [2012] was used.

2.1.3. Raschig-Tube

The Raschig-Tube (RT, Figure 1) is a glass cylinder containing many little glass rings ("Raschig-rings"; Invented by Fritz Raschig 1914) and a suitable absorber solution (here 100 ml of 1 - 1.5 M NaOH solution were used) in order to wet the surface of these rings. In this manner a large interaction surface is created, which is independent of the flow rate. This technique has been in use in many applications other than volcanic gas sampling, e.g. *Levin et al.* [1980] used RTs to capture

CO_2 from the flowing air and to determine the carbon isotopic composition. The RT technique is able to very efficiently capture acidic species in an alkaline solution allowing fast hydration and total dissociation. In this work the RT design was modified for an application in volcanic environments. The humidification of the Raschig rings is achieved by placing the RT on two cylinders (approximately the same length as the tube, see Fig. 1), one of which is connected to a 12 V direct current (DC) geared motor. In this way the RT is supported in a horizontal position and rotates at a constant speed (ca. 4 rpm). The whole set-up is placed on an aluminum base-plate, which can be aligned to a level position by three height adjustable feet to provide homogeneous wetting of all Raschig-rings. A Tygon tube leading to the pump is connected with a plain bearing adapter to prevent torsion of the tube.

In addition a second, smaller RT set-up was built ("small" Raschig-Tube – SRT), since it was found that the high efficiency of the "big" Raschig-Tube - BRT (see section 3) was not always needed. The SRT has a smaller volume (length: 8 cm, diameter: 7 cm) in comparison to the BRT (length: 13 cm, diameter: 10 cm) and due to its smaller size it is more suitable for field applications and transport. The device is small enough to place it in a 30 cm x 20 cm x 15.4 cm box, which can be closed to protect the rotating elements from ash and stones in volcanic environments. Beside this significant advantage a further important goal was the use of only 40-50 ml of solution instead of 100 ml for the BRT to obtain a more concentrated sample as well as to reduce the measurement time.

2.2. Sample pre-treatment/preparation

After the collection of a sample by DB or RT it is poured into an inert flask (polypropylen bottle). The volume of the bottle is less than 0.02% of the sampled air volume; therefore the contamination through the air in the headspace and also through the sample transfer can be neglected. For DB and RT samples we established a pretreatment procedure consisting of three main steps (section 2.2.1-2.2.3). The influence of each step on the quantification was tested to determine the right dose and to improve the sensitivity and accuracy for Ion chromatography (IC) and Inductively Coupled Plasma Mass Spectrometry (ICP-MS) - see section 2.3.

The pretreatment process of samples collected by FP differs from the others. The filters have additionally to be washed out by eluting the filter in 20 ml Milli-Q water (Millipore purification system, Bedford, MA, USA) in an ultrasonic bath for 120 minutes. An aliquot of the resulting solution was oxidized in order to transform reduced species into detectable forms (see section 2.2.2).

2.2.1. Neutralization of the Sampling Solution

The sampling solutions obtained by DB or RT have to stay alkaline in order to efficiently trap acidic gases. Having a strongly alkaline solution implicates matrix effects that reduce the detection limit and can distort the analytical results especially with regard to the here applied analytical methods (section 2.3). Aiming for the detection of very low halogen concentrations in the samples with several techniques the reduction of pH and thus of the sodium matrix effects is essential.

Whereas *Montegrossi et al.* [2001] used boric acid to neutralize the alkaline solution and to buffer the pH at 9.2, Dionex OnGuard II Cartridges are in widespread use to neutralize the samples. They contain styrene-based, strong acid resin in the H^+ form that allows an exchange of Na^+ ions with hydronium ions (H^+). In this work sulfur contamination was noticed by using these cartridges, preventing an accurate determination of low sample concentrations. Besides the contamination effect, the cartridges have a low capacity and are not re-usable what makes the preparation expensive. Therefore, an Anion Self-Regenerating Neutralizer 300 (ASRN 300) was installed and tested in this work. The ASRN 300 is a membrane-based electrolytic device that is able to remove the sodium ions by replacing them with hydronium that reacts with the hydroxide ions to form water. The net effect is the neutralization of the soda matrix and the conversion of the sample ions to a more ionized form in a weakly dissociated water matrix, which additionally leads to a change in density. It should be remarked that depending on the anion concentrations there is sodium resting in the neutralized solution. A possible sulfate contamination by the exchange membranes was investigated by neutralizing pure water and a 1 M NaOH blank solution two times. Anion concentrations, analyzed by IC, for pure water were still under detection limit and a contamination in the NaOH solution was not detectable in comparison to the blank contamination due to the commercial pellets (Merck; pc: 106462). Furthermore, the influence on dissolved species was tested by analyzing the NEC 4.3 sample at different stages of neutralization. The results showed no effect on chlorine and sulfur, but a remarkable difference for fluorine after the sample passed the ASRN four times. A possible explanation is that the pH drops with every run and fluorine starts to form the undissociated hydrofluoric acid (HF) or even minor amounts of bifluoride (HF_2) at a pH below 5, that can be reached based on the present anion concentration and the Na^+- H^+ exchange. The neutralization has to be performed carefully in order to avoid a negative impact on the anion concentrations.

2.2.2. Determination of Total Sulfur

After neutralization sulfur species have to be oxidized in order to determine the total sulfur concentration as sulfate that is quantifiable by IC. The most efficient way is the addition of

hydrogen peroxide (H_2O_2) [e.g. *Giggenbach*, 1975 or *Mioduszewski and Kress*, 2008]. *Mioduszewski and Kress*, [2008] compared the oxidation by H_2O_2 to the relatively inefficient O_2 aeration. During the reaction of sulfite with H_2O_2 the primary oxidation product is sulfate with a reaction rate constant in the order of $10^7 – 10^8$ $l^2mol^{-2}s^{-1}$ [*Maaß et al.*, 1999], whereas the oxidation of sulfide can form polysulfide intermediates depending on the pH [*Hoffmann* 1977]. In this study a waiting period of at least one night was abided to guarantee total oxidation. The highly reactive H_2O_2 causes baseline effects that can lead to an inaccurate quantification especially for anions with short retention times (e.g. fluoride). Additionally, H_2O_2 could damage the separator column [*Kerth and Jensen*, 1995] and should be only added in very small amounts. *Toutain et al.* [2003] attempted to remove excess H_2O_2 by warming up the solution gently to 30°C. However, any possible excess of the dissolved gases of interest should be avoided. Therefore we added a small amount of granular manganese dioxide (MnO_2) similar to *Beckman et al.* [1990]. MnO_2 acts as a catalyst for the H_2O_2 removal reaction ($2\ H_2O_{2\ (aq)} \rightarrow 2H_2O + O_2\ (g)$). It is insoluble in water and remains as powder in the sample. An inert filter has to be used when inserting the sample solution into the ion chromatograph. Moreover, before using the powder was washed several times to reduce contamination through other ions. The removal reaction was accelerated by sonication. Several tests were performed to investigate influences of H_2O_2 and MnO_2 on the chromatogram. Adding H_2O_2 to Milli-Q water nicely illustrates the baseline effects especially at the beginning of the chromatogram where the fluoride peak is located (see Figure 2). MnO_2 is able to remove these effects nearly completely.

2.2.3. pH adjustment

A high content of hydrogen carbonate anions and dissolved CO_2 can drastically interfere in the chromatogram with anion signals of interest. However, removing this influence is complicated because the eluent, used in the IC to carry the analyte in this work, consists of a bicarbonate carbonate mixture. This mixture provides a stable baseline in the chromatogram. In case the sample solution has a pH below 7 after application of the ASRN and thus the bicarbonate to carbonate ratio differs from the eluent, the detected signal can be influenced. Dissolved carbonate can form micro-bubbles of CO_2 within the suppressor and physically inhibit the exchange of Na^+ with H^+. The momentary higher fraction of Na^+ and the smaller quantity of H^+ relative to the rest of the sample eluting before and after results in a lower conductivity as described in *Novic et al.* [1997]. In our case, this effect exactly interferes with the chloride peak.

In this work, the influence of pH on the appearance of the bicarbonate peak was tested. The pH increase results in a shift of the peak to later times out of the chloride peak. At a pH about 8 the

bicarbonate peak often even disappears completely (see Figure 3). This suggests that at this pH the sample has the same bicarbonate carbonate equilibrium as the eluent. To increase the pH up to circa 8, a small amount of 0.1 M NaOH solution can be added. For example to raise the pH from 4 to 8 an addition of about 5 µl is sufficient and causes a dilution error of only 0.1 %. This increase in pH is also useful to avoid the escape of dissolved elements of interest in gaseous form. Hence pH adjustment is an important application for similar analytical set-ups to guarantee an accurate quantification of chlorine especially for low concentrations.

2.3. Analytical methods

This work focuses on IC that offers a fast and economical detection of many elements of interest (e.g. S, Cl, F, Br) in a wide concentration range. Since IC is not enough sensitive for an accurate quantification of very low concentrated elements, ICP-MS (Agilent 7500 CE, at INGV Palermo) was chosen to analyze for bromide and iodide in the neutralized samples. It was not possible to quantify fluorine from filters by IC due to the glycerol affecting the beginning of the chromatogram and overlapping with the fluoride peak. Alternatively fluorine concentration of FP samples is often quantified by the ion selective electrode technique [*Aiuppa et al.*, 2004]. This was also applied in this work for FP samples from 2010 and 2011. However, the problems related to the analysis of fluoride (by IC or by electrode) have never been adequately discussed (e.g. the influence of organic compounds for IC analysis, or the effect of the complexes of aluminum for ion selective electrode determination) and therefore it is difficult to estimate an uncertainty. The IC system was an ICS1100 Dionex (at INGV Palermo) equipped with a 75 µl sample loop, a Dionex AS14A column that requires a 8.0 mM Na_2CO_3/1.0 mM $NaHCO_3$ eluent (a flow of 1 ml/min was used), suppressor and conductivity detector. For every IC session fresh eluent was prepared and the IC was calibrated using the same standard solutions for all the sessions. When the instrument was turned on, at least one hour was waited to be sure that total conductivity (conductivity caused by the suppressed eluent) was stabilized. Afterwards, 7 standard solutions were analyzed, Milli-Q was inserted to test memory effects and possible contamination through the highly concentrated standards. No effects were found. For each sample the calibration levels were chosen depending on the detected concentration range in order to obtain the best fit in that range. The accuracy of every session was determined with analysis of certified reference materials (Ontario-99 and Lethbridge-03) and combined with the precision (standard deviation of 10 analysis of each calibration standard) to estimate the uncertainty of each analysis. The uncertainty of the ICP-MS analysis was obtained by performing 5 replicates of each sample yielding a standard deviation.

The BRT, SRT and DB samples were additionally analyzed for dissolved CO_2 by Titration (Orion 960 autochemistry system). The uncertainty of the results was determined experimentally by analyzing prepared standard solutions several times. The blank concentration or, in the case of CO_2, the atmospheric contribution $c_{blank/atm}$ to the measured total analyte concentration c_{tot} increases with a decreasing amount of water in the sample solution. To account for this effect $c_{blank/atm}$ is multiplied by the measured ratio of the sodium concentrations before ($c(Na^+)_{before}$) and after ($c(Na^+)_{after}$) sampling to obtain the corrected analyte concentration c(analyte):

$$c(\text{analyte}) = c_{tot} - c_{blank/atm} \times \frac{c(Na^+)_{before}}{c(Na^+)_{after}} \quad (1)$$

Alternatively, the sample solution can be weighted before and after sampling to estimate the evaporation and thus obtain the correction factor for the blank concentration. The atmospheric fraction of total dissolved CO_2 was estimated by the mixing ratio of CO_2 in the air [http://www.esrl.noaa.gov/gmd/,], the volume of sampled air, atmospheric pressure and temperature, and the volume of sampling solution (see equation (2)). Also for the FP measurements the blank effect was corrected by analyzing not exposed but impregnated filters. Although for most concentrated samples the blank effect is negligible (see Table 2), all analytical results were processed in the same manner. For fluoride and bromide blank concentrations were below the detection limit of the instruments, which is about 1 µmol/l and 3 nmol/l respectively.

3. Sampling efficiency - Theoretical background and empirical evaluation

To demonstrate the sampling characteristics of the various active alkaline traps one can consider the development of the molar concentration c_i of an element i in the respective solution. c_i depends on the molar gas fraction χ_i of the element in the sampled air, the sampling flux Q, the sampling time t, the amount of solution V_w, the ambient temperature T and pressure p, and the ideal gas constant R:

$$c_i = \frac{\chi_i Q\, t\, p}{V_w R T} \quad (2)$$

Figure 4 shows the evolution of c_i in an arbitrary high concentrated NaOH solution for different concentrations of a divalent species in the air at a given atmospheric pressure and for the different instruments assuming 100 % absorption efficiency (filter packs are not taken into account since the amount of sampling solution on the filter is highly variable and could not be reproduced). The element concentration in the RT sampler increases fast with the sampling time in comparison to the DB, due to the high applicable flux and the smaller amount of sampling solution. The dashed saturation line indicates the point in time where one mole of a species would have reacted with two mole OH^- ions as it occurs during the dissolution and dissociation process. This simplified

assumption roughly illustrates the threshold for a 1 M NaOH solution that should not be exceeded during sampling since the efficiency cannot be guaranteed anymore.

A theoretical approach for comparing absorption characteristics was developed in order to calculate the absorption efficiencies of the three sampling set-ups (DB, BRT and SRT). Only the efficiency with respect to CO_2 was investigated, since this gas has a low effective solubility [*Sander*, 1999] and a low acidity in comparison to the other species of interest that degas from fresh magma. Being able to capture CO_2 efficiently, allows to capture all the other, more soluble and stronger acidic species in the solution as well. Filter-packs are not considered in this approach because the absorption features are difficult to describe also due to the strong influence of chemical reactions within the $NaHCO_3$ solution.

The solubility depends on pressure and temperature [e.g. *Bowyer and Woolf*, 2004], therefore the sampling efficiency can change depending on the sampling sites. In the following calculations, the efficiency is derived for laboratory conditions (T = 25°C and p= 1013 hPa).

3.1. Sampling efficiency – Drechsel Bottle

The estimate of the absorption efficiency of DBs is based on Fick's law stating that the trace-gas flux j is proportional to the concentration gradient of the species between aqueous and gaseous phase. Assuming a constant flow density for the bubble induced gas exchange with a homogenous flow perpendicular to the bubble surface it is sufficient to consider a 1D transport model. In this case j can be expressed as a function of the concentration difference Δc between aqueous and gaseous phase. This leads to the standard equation for gas liquid exchange where w represents the transfer velocity that summarizes the effects of molecular (and turbulent) diffusion [*Jaehne and Haußecker*, 1998]:

$$j = w \cdot \Delta c \tag{3}$$

With the dimensionless Henry's law constant $\alpha = c_a/c_g$ (where c_a and c_g denote the gas concentration in the solution and in the gas phase, respectively) the mass balance of a bubble with the volume V_b ($\frac{4}{3}\pi r^3$) and the surface A_b ($4\pi r^2$) can be written as:

$$V_b \frac{\partial c_g(t,t')}{\partial t'} = A_b w\left[c_a(t) - \alpha c_g(t,t')\right] \tag{4}$$

Here t is the sampling time, t' age of the bubble in the water ($0 \le t' \le \tau$), τ the total lifetime of a bubble, $c_g(t, t')$ the concentration of a species in the bubble, and $c_a(t)$ the concentration of a species in the solution. It is assumed that $c_a(t)$ does not change during the residence time of the bubble and

only depends on the sampling time. Assuming an instantaneous dissociation and depletion of the hydrated species, justified by the high alkalinity of the solution, $c_a(t)$ can even be set to 0 in good approximation. Thus the absorption efficiency is considered to be driven by the physical solubility and only counts as long as the chemical dissolution takes place much faster than the physical. The initial condition $c_g(t'=0) = c_{g0}$ leads to the expression for the concentration in a bubble with a radius r that passed the solution within the time τ:

$$c_g(\tau) = c_{g0} \exp\left[-\frac{3w\tau\alpha}{r}\right] \tag{5}$$

τ can be calculated based on the height h of the liquid column and the bubble velocity v_b, derived from the equilibrium of buoyancy force F_B and drag force F_D on the bubble. According to the approach from *Roghair et al.*, 2011 one has to account for the gas fraction β and the change of the drag coefficient C_D for a bubble in a swarm to calculate τ in dependence of h, r, β, C_D, and the gravitational constant g (9.81 m/s^2):

$$\tau = \frac{h}{v_b} = \frac{h}{\sqrt{\frac{8}{3}\frac{rg(1-\beta)}{C_D}}} \tag{6}$$

Assuming a constant bubble emergence frequency f (number of bubbles/min) an increase of the sample flow leads to an increase of the bubble radii:

$$f = \frac{Q}{V_b} \rightarrow r = \sqrt[3]{\frac{3}{4\pi}\frac{Q}{f}} \tag{7}$$

Finally, inserting equation (6) and (7) in (5), the absorption efficiency E can be defined as:

$$E = 1 - \frac{c_g(\tau)}{c_{g0}} = 1 - \exp\left[-3w\alpha h\sqrt{\frac{\pi C_D f}{2gQ}}\right] \tag{8}$$

The absorption efficiency mainly depends on the:

- transfer velocity w: 0.34 cm/s for CO_2 in 1 M NaOH at 25°C [*Siegenthaler and Muennich,* 1981]
- physical solubility of a species in 1 M NaOH: $\alpha_{CO2,1MNaOH} = 0.6$, calculated after the method proposed by *Danckwerts* [1970] based on the physical solubility of CO_2 in water , $\alpha_{CO2,H2O} = 0.83$ [*Sander*, 1999]
- bubble emergence frequency f: estimated by photo-optically determination of the mean bubble radius at Q = 1 l/min
- height of the liquid column h: typically 10 cm for the applied round-bellied DB's filled with 100 ml of liquid [*Liotta et al,* 2012]

- Drag Coefficient C_D: 2 for $\beta \approx 0.1$ [*Roghair et al.,* 2011]
- applied air sample flow Q

As a consequence, applying a higher flow rate causes larger bubbles that rise faster and have a shorter residence time, leading to a less efficient gas uptake. For instance, assuming w, α, and C_D as defined above, Q = 1 l/min and r = 0.2 cm (at Q = 1 l/min) leads to the absorption of 88.2% of CO_2, whereas an increase to Q = 2 l/min reduces the absorption efficiency to 80.0%. In practice, not only r but also f can change with the flow and the form and size of the bubbles show rather high variations. The frit pore sizes may have a relatively low impact on this effect since the bubbles formed at the frit coalesce rapidly [*Gage,* 1960], though we could observe a considerable difference for the two applied frits (Figure 5).

3.2. Sampling efficiency – Raschig-Tubes

To derive the theoretical absorption efficiency of the Raschig-Tube the basic approach of *Levin* [1978] was modified. The Raschig rings have an internal diameter of 5 mm (external diameter: 6 mm) and a length of 6 mm (total ring surface $A_r = 2.07$ cm^2) and are deposited along a length L within the tube. The mean density of the rings in the tube is assumed to be $\rho = 3.6$ rings/cm^3.

The concentration of trace gas in the air coming out of the tube depends on the time τ_r an air parcel needs to pass the section with the rings. This time depends on the length and the flow velocity that is defined by the air flow Q and, since the tube volume V_R is reduced through the Raschig rings, by the effective cross-sectional area A_{eff} of the RT:

$$\tau_r = \frac{L \cdot A_{eff}}{Q} \tag{9}$$

In this way the mass balance for the gas exchange in the RT can be determined comparable to the bubble induced absorption with the assumption of an instantaneous depletion of hydrated species:

$$V_R \frac{\partial c_g}{\partial t} = A_r \cdot \rho \cdot V_R \cdot w \cdot \alpha \cdot c_g(\tau) \tag{10}$$

Solving the differential equation leads to the gas phase concentration of a species after passing the tube [*Levin,* 1978]:

$$c_g(\tau_r) = c_g(0) \cdot \exp\left[-A_r \cdot \rho \cdot w \cdot \alpha \cdot \tau_r\right] \tag{11}$$

Assuming w, α, ρ, and A_r as defined above, Q = 5 l/min, L = 13 cm, and $A_{eff} = 64$ cm^2 leads to the absorption of 99.99 % of CO_2.

3.3. Sampling efficiency - theoretical and experimental comparison

Figure 5 shows a comparison of the theoretical absorption efficiency for the DBs with different frits and the SRT and BRT. The plots show the fraction of captured CO_2 after passing the absorber device as a function of sample air flow. Increasing the flow reduces the residence time of an air parcel or increases the bubble size and thus leads to lower absorption efficiency. The variation of the bubble radius for DB 1 (r = 0.15 cm) and DB 2 (r = 0.2 cm) indicates different frits which generate different bubble sizes at the same flow (Q = 1 l/min).

In order to compare both sampling set-ups, qualitative atmospheric test measurements were performed by installing a CO_2 infrared gas analyzer by Edinburg Sensor after the air passed the instruments. Figure 5 summarizes these measurements for two DBs with different frits and the RTs. The uncertainty is represented by the standard deviation. Applying higher fluxes, the efficiency of DB 1 decreases rapidly whereas nearly no effect can be recognized for the other instruments. In general, the DB shows higher standard deviations in comparison to the RT. This effect is probably caused by bubble size variations that cause a high variability of the efficiency and thus of the detected concentrations.

The results of the RTs are within their uncertainty in good agreement to the theoretical approach. The efficiency of DB 2 should decrease with higher fluxes but the model prediction could not be confirmed by the measurement demonstrating the challenge and difficulties to theoretically describe such a system. For more detailed studies we refer to e.g. *Calvert and Workman* [1961], *Simonnet et al.* [2007], or *Roghair et al.* [2011]. A higher flow range could not be investigated since the increasing bubble size leads to an overflow of the sampling solution.

As described in equation (11), the theoretical efficiency does not directly depend on the amount of solution inside the RT. It is only of importance that enough liquid is provided to humidify all the rings. Moreover, the amount of solution used for sampling has an influence on the capacity and the concentrations of the elements inside. It can also affect the effective interaction surface when an irregular flow velocity creates a dead surface or when some rings are clogged by solution.

4. Field sampling

Three sampling campaigns were conducted at Stromboli and Etna (Italy) in 2011 and 2012. Table 2 gives an overview on sample names, applied flows, sampled air volumes, and analytical results allowing to evaluate the various techniques and the sampling conditions. Sampling locations were chosen depending on the local wind conditions and accessibility to the crater area.

4.1. Mount Etna

During field sampling on Mt Etna all four active summit crater - North East Crater (NEC), Bocca Nuova Crater (BN), Voragine (VOR) and South East Crater (SEC) - were in a state of quiescent degassing. Samples were taken at the rim of BN and NEC. NEC and BN were characterized by large gas emission during our field studies. VOR and SE crater showed only small gas emission in this period. A week after sampling slight Strombolian activity started inside the BN accompanied by an increase in the seismic signal [http://www.ct.ingv.it] and later on a small lava effusion inside the crater.

On June 26, 2012 samples were taken at the NEC applying DB, FP, SRT and BRT simultaneously. As mentioned earlier filter packs saturate quickly and therefore a shorter sampling time than for other instruments (DB, SRT, BRT) has to be applied. One FP sample was taken at the beginning and one at the end of the measurement, each for about 5 minutes. Moderate westerly wind provided high plume gas concentration at the NEC. Sampling directly at the rim, the plume age can be estimated to <1 minute. On June 27, 2012 the instrumentation was applied on the rim of BN. Meteorological conditions had changed to higher humidity and a slight breeze led to a straight up plume rise. The location that had to be chosen accommodated fumaroles that could have contaminated the measurements, due to the variable wind directions.

For Mt Etna, a small set of DB and FP samples collected during the last two years was evaluated in this work as well. However, DBs with unknown efficiencies in combination with a diaphragm pump and a rotameter has been used in 2010 and 2011. This introduces a higher error in particular for the CO_2 determination, where the fraction of dissolved CO_2 in the sample caused by the atmospheric background is calculated based on the sampled air volume.

4.2. Stromboli

The explosive activity at Stromboli was relatively weak in September 2011 as well as on the first day of the June 2012 campaign. On the following two days in June 2012 a slight increase in activity as well as wind speed could be recognized. A significant amount of ash released by the explosions reached the sampling location. To estimate atmospheric contamination (for instance sea spray) a blank measurement was performed at sea level in September 2011.

On June 20 and 21, 2012 excellent weather and wind conditions prevailed and provided high concentrated samples. Samples were taken at the southwest Pizzo crest. A moderate wind from North-East blew the plume directly over the rim situated 100 m above the craters next to Pizzo Sopra la Fossa. Based on the meteorological parameters (Table 1) the sampled plume ages were estimated to be <1 min.

At both locations, the samples were taken by all direct sampling instruments described in section 2. In order to compare effects of the sampled air volume on the results, flow and runtime were varied. The weather conditions prevented a significant BRT sample at Stromboli (see section 5.1) on June 19, 2012. Table 2 gives an overview on sample names, applied flows, sampled air volumes, and analytcial results. For some samples, a 1.5 M NaOH solution (instead of 1 M NaOH) was used to achieve a long sampling time by avoiding early saturation. Therefore high concentrations were obtained and less abundant elements could be detected.

5. Results and Discussion

5.1. Molar sulfur to halogen ratios (S/[X])

Analytical results were processed to correct for blank effects. For the DB, SRT and BRT samples the blank concentration of the NaOH solution was subtracted taking into account dilution and evaporation effects (see section 2.3.). The samples STR 0.1, STR 1.1, and STR 1.2 do not deviate from the blank concentrations and consequently are not considered in the further evaluation. In the following, only element symbols (S, F, Cl, Br, I) are used for sulfur and halogens to express the ratio.

To indicate the plume dilution at the sampling sites Table 3 summarizes the concentrations of volcanic gases in the air derived for the various days based on the DB and RT samples. The concentration for each element has been computed solving equation (2) for χ_i. The values facilitate the interpretation of the sample results with respect to the volcanic gas concentration at the sampling sites. Up to 30 times higher element concentrations were present at Mt Etna in comparison to Stromboli due to the stronger plume of the former and the possibility of a closer approach to the emission source. The low molar fraction of volcanic gases on September 29, 2011 and June 19, 2012 indicate the adverse meteorological conditions at those days and are related to the low analyte concentrations close to the blank.

Table 4 shows the molar CO_2/S, S/Cl, S/F, S/Br and S/I ratios obtained during this work for the various techniques and for each sampling site.

5.1.1. Results - Mount Etna

Plume gases from Mt Etna are admixtures of compositionally distinct emissions from the various summit craters [e.g. *Pennisi and Le Cloarec*, 1998; *La Spina et al.*, 2010; *Rizzo et al.,* 2013]. This is consistent with the molar ratios obtained in this work (see Table 4). Except for the low concentrated iodine results, the molar S/[X] ratios are in good agreement for all instruments applied at Mt Etna. The ratios fit quite well within the uncertainty indicating reliable results. Table 2 includes some FP

samples containing a significant analyte concentration in the 3rd stage of the pack and thus are labeled and not considered for the discussion of the results. They are solely taken up to demonstrate the saturation effects in Figure 9 and 10 which are discussed in the last paragraphs of this section.

Figure 6 presents the S/Cl ratios obtained by the various techniques together with the sampled air volume to point out the different sampling properties. Regarding the results for each instrument a sampling volume dependency, e.g. due to selective absorption, can be excluded (see also Figure 9). Obtained S/Cl values at NEC for the respective sampling technique are 1.89 ± 0.11 (DB), 1.85 ± 0.08 (SRT), 1.83 ± 0.08 (BRT), and 1.79 ± 0.18 (FP) at NEC. Especially for NEC a good agreement between all traps can be observed. The minor discrepancies for the FP data from the other instruments could be caused by the inability of Filter-packs to capture H_2S *[Mioduszewski and Kress*, 2008]. Transferring this assumption to our results based on a SO_2/H_2S ratio of 20 [*Aiuppa et al.*, 2005b] the FP ratio increases to 1.88 ± 0.19 which is consistent with the DB, SRT and BRT (S/Cl = 1.83-1.89, see Table 4). The S/Cl ratios for BN instead show relatively high variations (DB: 3.5 ± 0.7, SRT: 2.6 ± 0.1, BRT: 3.2 ± 0.2, FP: 3.1 ± 0.9) that are obviously not caused by instrumental differences but rather by the adverse meteorological conditions and the high amount of fumaroles around the crater rim that could affect the measurements.

Looking in more detailed at our dataset Figure 7 shows the concentrations of chlorine (marked in blue) and bromine (marked in green) as a function of the molar sulfur concentrations for each applied type of alkaline trap. Again the good accordance of the S/Cl and additionally of the S/Br ratios for the NEC samples is illustrated by a linear regression respectively (forced through zero). The resulting mean S/Cl and S/Br values are displayed as an orientation. For S/Br the DB samples result in a slightly lower ratio (mean S/Br: 1015 ± 66) than SRT (S/Br: 1167 ± 52), BRT (S/Br: 1206 ± 63), and FP (S/Br: 1123 ± 38) results (see also Table 4).

Comparing the obtained S/Cl values for NEC with previous studies, significant differences can be found to FTIR measurements by *La Spina et al.* [2010] and *Burton et al.* [2003] that both found a S/Cl ratio of 2.9 but also to FP measurements by *Martin et al.* [2008] and *Aiuppa et al.* [2005a] resulting in a S/Cl value of 0.9 and 1.1. For S/Br the obtained ratios are slightly lower than the value obtained by *Aiuppa et al.* [2005a] (S/Br: 1344) and much higher than the S/Br ratio of 60-71 given by *Martin et al.* [2008]. Differences found between the various data sets might be caused by changes in volcanic activity but also by the sensitivity of the various applied techniques for different compounds. The FTIR method for instance determines chlorine only in the gas phase and as HCl molecule. Using alkaline traps instead, the trapped gaseous, liquid, and solid compounds are quantified as a total elemental concentration. Therefore it would be of high interest to undertake joint field measurements and simultaneous sampling in a future work.

In Figure 8 the molar sulfur, chlorine and bromine concentrations for the BN samples are compared. The detected S/Br ratios in the plume of the BN crater show a mean of (2000 ± 214) for DB, (1925 ± 198) for SRT, and (2217 ± 212) for BRT. The FP result (S/Br: 3128 ± 581) is probably the most error-prone due to the sampling location and the short sampling time that is more susceptible to temporary variations of degassing dynamics or of meteorological conditions (e.g. wind direction). The S/Br and S/Cl ratios are roughly up to two times lower at the NEC in comparison to the BN. This points to a different fractionation processes in the plumbing system and the gas phase for each crater or a variation of the depth of degassing as suggested by *La Spina et al.* [2010]. It is challenging to compare the ratios for BN with other works since most of them show even higher variations than our results or measured at another location (e.g. next to the Voragine crater located adjacent to BN). In the recent past *Martin et al.* [2008] and *Aiuppa et al.* [2005a] determined mean S/Br ratios of 67 and 3102 for the quiescent degassing plume of the Voragine crater in 2005 and 2004 respectively.

Figure 9 and 10 display ternary diagrams for the results at NEC and BN (S, Cl, F) obtained in this work together with results from other studies [*La Spina et al.*, 2010; *Martin et al.*, 2008; *Aiuppa et al.*, 2002, 2005a; *Burton et al.*, 2003].

For BN (Figure 10) a shift to a lower halogen fraction in comparison to NEC (Figure 9) can be seen. The ternary diagram for NEC repeats the good accordance for the applied instruments including the results for fluorine. However, the discrepancies to ratios obtained in other works come clear especially for FP measurements. In general BN results show a broader distribution for reasons of influences through fumaroles that are depleted in HCl and HF [*Liotta et al.*, 2010] and therefore can also shift the results towards higher S/[X] ratios. But also the sensitivity of the BN plume composition to the frequent changes in activity [*Aiuppa et al.* 2002] has to be taken into consideration. The qualitative comparison to published results shows in some degree a good agreement but also a slight shift towards higher chlorine and fluorine values for ratios given by *La Spina et al.* [2010], *Burton et al.* [2003], and *Aiuppa et al.* [2002].

To investigate the effects of saturation on FP measurements the respective samples are included as asterisks in Figure 9 and 10. They represent saturated filter pack measurements performed in 2010 and 2011 where filter C (last filter in the row) showed comparable sulfate concentrations to filter A or B. The diagram nicely illustrates the falsification of molar ratios when the filters are saturated. As an orientation, non-saturated filter pack measurements taken during the same time period are displayed to exclude a volcanic caused change of the gas composition. Once a filter is saturated, the

trapping process starts to be selective. Thus stronger acids are overestimated explaining the observed tendency to chlorine and fluorine in the ternary diagrams (asterisks in Figure 9 and 10) for saturated filter pack samples (see also *Mioduszewski and Kress* [2008]). The two samples in Figure 9 located even further below the others were "oversaturated" with much higher sulfate concentrations in filter C than in filter A and B and thus confirm the trend.

Unknown mixing of results from saturated and not saturated filter pack sampling can lead to a misinterpretation of data, for instance lower S/Cl and S/F ratios caused by a saturation effect could be interpreted as tendency for gas composition changes depending on the stages of an eruption. In fact, since sulfur is less soluble in magmas than chlorine and fluorine gas compositional changes from sulfur rich to sulfur depleted gases can mainly be ascribed to the degassing dynamics of the magmatic bodies [e.g. *Spilleart*, 2006; *Aiuppa*, 2009]. In view of that it is very important to validate S/[X] ratios. Considering the systematically significant low gas phase S/[X] ratios in *Martin et al.* [2008], an explanation could be the applied flow and sampling time, which seems too high based on our experience made with a three-stage gas filter and thus could lead to saturation effects and to an inefficiency due to the fast movement of the sampled media. However, the application of a particle filter in front of the FP samplers is not able to explain such high discrepancies since the molar amount of the species in the collected particles is negligible with respect to the molar amount in the gas phase [*Martin et al.*, 2008].

5.1.2. Results - Stromboli

At Stromboli Island large short term variations in the gas emissions were observed in the past due to the strombolian activity [e.g. *Burton et al.*, 2007]. It should be noted that the molar sample concentrations of alkaline trap samples represent a mean value over explosive and passive degassing during the sampling time.

Comparable to Figure 6 for Mt Etna, Figure 11 shows the obtained S/Cl ratios as a function of sampled air volume for each applied sampling technique. At Stromboli DB (S/Cl = 1.59 ± 0.18) and SRT (S/Cl = 1.61 ± 0.03) ratios agree quite well within the uncertainty. Only a slight deviation to lower S/Cl ratios can be observed for DB samples with the exception of sample STR 0.2 from 2011 where a ratio of 1.8 ± 0.2 was found. It should be noted that STR 0.2 has relatively low analyte concentration, whereas the SRT samples have partly a more than 13 times higher analyte concentration than the DB samples taken over the same sampling time and at the same location (see Table 2).

Filter pack measurements are systematically lower and show much larger scatter for S/Cl (1.25 ± 0.11, see also Table 4) although the uncertainty based on the analysis is lower. Either chlorine may

be overestimated or sulfur is underestimated for all FP samples. The effect of H_2S on the filter packs, as for Mt Etna, is not sufficient to completely explain the deviations in spite of the presumable higher H_2S fraction (SO_2/H_2S = 15, [*Aiuppa et al.*, 2005b]). The H_2S loss leads to a S/Cl increase of roughly 7 % which is not sufficient to explain the high difference to the DB and SRT samples of 28 %. The same effect should also be noticeable for the S/Br ratios but this is not the case as it can be seen by confronting the molar sulfur, chlorine, and bromine concentrations (Figure 12). Rather conspicuous are the systematic lower S/Br ratios obtained by the DB. The mean S/Br ratio of the DB samples (673 ± 136) is almost half of the ratio resulting from FP (1287 ± 119) and SRT (1279 ± 68). This tendency is also found for Mt Etna samples although not to this extent. Possible explanations are the low concentrations and thus systematic effects for the analysis near the detection limit or the selective dissolution of bromine species in the DB. Though the FP concentrations seem to be in the same concentration range, they represent the mean value over three filters where for most samples filter A contains much higher molar concentrations with over 90% of the dissolved species (see Table 2).

The systematic lower S/Cl ratios for filter packs suggest a non-volcanic chlorine contribution or a selective dissolution of gaseous species in the filter packs. A possible contamination could be caused by the influence of sea salt aerosols. Relevant sea salt aerosol components are Cl^- (55 wt%), SO_4^{2-} (8 wt%), Br^- (0,19 wt%) and I^- (10^{-4} wt%) [*Seinfeld and Pandis,* 1998] and a contribution would lead to a decrease in both S/Cl and S/Br ratios. Further possible contamination factors could be solid ash particles released by the volcano (especially during explosions). In fact, *Mather et al.* [2004] and *Liotta et al.* [2006] found such a mixture between volcanogenic and sea salt aerosols at Stromboli, though the analysis of the pump inlet filters does not indicate non-dissolved aerosols in any instrument. Whereas the capture of aerosols by filters with various pore sizes is partly known and applied in other studies [e.g. *Sedlacek et al.*, 1984 or *Anlauf et al.*, 1985], the particle uptake efficiency in the DB and the RT is not clarified yet. More detailed measurements of the particle phase need to be done to prove or disprove these suggestions.

For the S/F ratio we obtained relative consistent results between SRT (16.2 ± 0.8 and 18.4 ± 1) and DB (12.7 ± 0.7 and 13.7 ± 0.7) accounting for the challenging quantification. The improvements in the sample pretreatment made an accurate quantification of fluoride by IC possible, whereas the FP samples could not be analyzed due to organic impurities of the filters as mentioned above.

A comparison to published ratios reflects the challenge for plume sampling at Stromboli since a high variability exists probably caused by low gas concentrations, the mixture of various craters and the difficulties to approach the emission source entailing problems for most measurement

techniques. Figure 13 displays the obtained S/Br and S/F ratios in comparison to the results by *Allard et al.* [2000] where the ratios were determined in dependence on the state of activity as indicated in the legend. Even if the ratios obtained by SRT are in the range of the given results for medium and high activity, the studies are hardly comparable due to the time difference of more than 15 years and the frequent change in activity of the Stromboli volcano.

Aiuppa and Federico [2004] used passive samplers (diffusive tubes; DT) to measure a mean S/Cl of 1.2 in a post-explosion phase 2003, but had to deal with high variations (0.3-8.8) during the investigated period (April-September 2003). Due to the even higher variations of S/F (0.3-17) no mean value is given by the authors. *Burton et al.* [2007] gives a range of 1-1.5 for the molar SO_2 to HCl ratio during quiescent degassing and an increase up to 2.5-4.7 for explosions determined with an OP-FTIR. The data of DB and SRT result in a mean S/Cl (standard deviation) of 1.6 (± 0.1) and fit quite well to this range, respecting that a mean value for passive degassing and explosions is determined. Recently, *La Spina et al.* [2013] confirmed a range from 1.4-1.9, depending on the crater, by an OP-FTIR scanning system.

The ternary diagram (Figure 14) confronting S, Cl, and F for every sample shows a rough agreement to measurements by *Allard et al.* [2000]. Whereas the DB and the SRT results are very similar, differences for the Polytetrafluoroethylene bags in combination with Draeger tubes [*Allard et al.*, 1994] and diffusive tube measurements [*Aiuppa and Federico*, 2004] are conspicuous. A simple explanation could be the exceptional moment of activity (post-explosion phase) concerning the work by *Aiuppa and Federico* [2004] even if problems in sampling (e.g. passive samplers trap species with different efficiency depending on their acidity [*Witter et al.*, 2004; *Mioduszewski and Kress*, 2008] and analysis for the applied techniques cannot be excluded.

5.2. The S/I Ratio

The iodine concentrations in most of the samples are above the detection limit of ICP-MS (≈ 10^{-9} mol/l). The results of the S/I ratios for NEC range from $4.6 \cdot 10^4$ to $18 \cdot 10^4$, depending on the sampling instrument. Our FP results (mean: $1.8 \pm 1.2 \cdot 10^5$) are in agreement with the only reported mean molar S/I ratio ($2.5 \pm 2.5 \cdot 10^5$) for NEC over 2004 by *Aiuppa et al.* [2005a]. However, DB ($4.6 \pm 0.3 \cdot 10^4$), SRT ($8.2 \pm 0.4 \cdot 10^4$), and BRT ($6.5 \pm 0.4 \cdot 10^4$) show substantially lower S/I values. This holds also true for BN where we found a S/I range from $5.0 \cdot 10^4$ (BRT) to $14.5 \cdot 10^4$ (FP).

At Stromboli volcanic iodine was detected for the first time. The resulting S/I ratios are between $1.1 \cdot 10^4$ (DB) and $28.4 \cdot 10^4$ (FP) representing a first range to estimate the amount of iodine released by the craters at Stromboli.

5.3. The CO_2/S Ratio

In general, CO_2 to S or SO_2 ratios of volcanic plumes are very sensitive for changes in the volcanic system [e.g. *Shinohara et al.*, 2008] but show a high uncertainty caused by the measurement techniques (mostly in case of non-spectroscopic in-situ techniques) and the high background concentrations (in the case of CO_2). Our first approach to determine CO_2/S by the applied alkaline traps does not represent an exception.

Most significant results were obtained for the NEC samples (high plume concentrations, less fumarole contribution) resulting a range of 3.6 to 7.5 (mean: 6.2 ± 2.6) for CO_2/S. Our results can be compared with recent gas composition measurements by other authors under the restriction that our ratios include H_2S and other sulfur species that are captured and have a stake in the so declared CO_2/S ratio. But considering a proportion of $SO_2/H_2S = 20$ for Etna and 15 for Stromboli [*Aiuppa et al.*, 2005] the contribution of H_2S to total sulfur (ca. 5-7 %) is relatively low.

E.g. *La Spina et al.* [2010] measured a range of 1.3 to 3.2 (CO_2/SO_2) for NEC and 2.9 to 10.9 for the central craters (Voragine and BN) by OP-FTIR. *Shinohara et al.* [2008] instead measured ranges of 3 to 14 for NEC and 15 to 30 for BN applying the MultiGAS technique. Our NEC data roughly fits to the ranges given by other authors.

The results for BN instead show a large distribution (CO_2/S = 26 - 73) and conspicuous deviation to published data. This could be caused by an affection of fumaroles at the sampling location and the challenging access to the BN plume on June 27, 2012 (high CO_2/S for SRT and BRT).

At Stromboli our results represent a mean value over few explosions and passive degassing. Regarding only the samples with a high volcanic fraction, our molar CO_2/S ratios show a range of 11.8 (SRT) to 16.4 (DB) and fit to published ratios. *Burton et al.* [2007] detected CO_2/SO_2 values from 7.8 to 20.7, applying an OP-FTIR. *Aiuppa et al.* [2010] confirmed these values roughly with long-term MultiGAS measurements. The authors give a mean molar ratio of 5.7 for the quiescent degassing bulk plume and 21.5 for the syn-explosive plume. *La Spina et al.* [2013] determined a mean CO_2/SO_2 ratio of 6.2 to 11.3 distinguishing the different craters.

5.4. The BrO/(total-Br) Ratio

For interpretations of the MAX-DOAS results in combination with direct sampling results, the probably dominant fraction of acidic bromine compounds (i.e. HBr) is assumed to dissolve in the alkaline sampling solution and therefore the result should be close to the total molar amount of bromine species (Br_{total}). Moreover, total sulfur is equated with SO_2 to combine the BrO/SO_2 ratios by the MAX-DOAS with the Br/S ratios obtained by direct sampling. For the mean Br/S ratio only

RT samples are considered. In this way a rough estimation for the molar BrO to Br_{total} ratio is obtained.

Table 5 illustrates the comparison of the results. At Mt Etna's craters the MAX-DOAS measurements were performed close to the vent at the crater rim. Here, a less diluted plume can be found and results agree well with former model studies for Etna by *von Glasow* [2010]. For NEC, a BrO/Br ratio of about 0.03 is obtained. The ratio of 0.06 at the BN crater can be explained with the structure of the crater that allows the plume much faster to mix with surrounding atmosphere than at the NEC. At Stromboli the MAX-DOAS measurements took place on the crater rim on July 19, whereas on July 20 and 21, 2012 the instrument was placed near to the harbor (air-line distance to the craters ≈ 1.5 km). The measurement sites and the wind speeds allow to estimate the plume age and several plume ages could be investigated by pointing the instrument in different azimuth angles into the plume. Assuming a constant Br/S ratio for these days, a BrO/Br ratio of about 0.071 is determined for the plume short after its release. The fraction increases for a plume age of about 4.5 min up to 0.108 and decreasing to 0.075 during the following 75 min. The rather high BrO fraction in the early plume indicates rapid bromine activation, probably due to the lower density of the plume and therefore a faster mixing with the surrounding atmosphere accelerating the reaction mechanisms in contrast to the plume at Mt Etna. In comparison to the model results by *von Glasow* [2010] the total final BrO/Br ratio is in good agreement, whereas the measured high BrO fraction in the early plume is not predicted by the model.

However, the models are based on input data fitted for Mt Etna and its characteristic plume composition, but also many other variables like the dilution rate with surrounding atmosphere or the presence of aerosol particles play a major role in the formation of BrO and should be specified for each volcano for accurate predictions [*Bobrowski et al.*, 2007].

6. Conclusions

Three sampling techniques (FP, DB, RT) were tested and applied in order to determine the molar gas ratios of acidic gases in volcanic plumes. All the tested techniques are based on the use of an alkaline solution that react fast with acidic gases and trap them as dissociated ions. Among several aspects explored in this paper, here we focus on the main strengths and weaknesses of each technique:

- FP represents the technique which is most practical in the field, since it requires only unbreakable materials that can be easily transported everywhere without particular precautions. Its trapping capacity is however limited by the amount of solution that each

filter can keep. If the total amount of acidic species which passed through the filters exceeds the maximum trapping capacity of the filter package, large errors due to the ineffective sampling can occur. Such a problem particularly affects sulfur versus halogen ratios; A further disadvantage is that CO_2 cannot be trapped by FP without quickly exceeding the trapping capacity. Note that for each FP measurements attention needs to be paid to the relative abundances of trapped species on each filter. As a general rule the relative amounts on the last filter should be negligible compared to the total amount of the analyzed elements. FP results should always be presented in combination with concentrations obtained on each filter to demonstrate the significance of the results. In addition, the analytical procedure is relatively laborious and inferior to other sampling techniques for fluorine determination.

- DB needs glassware and solutions to be transported in the field. This requires a certain attention during transport and start-up of the sampling. When e.g. wrapped in foam rubber DB can easily be placed in the field. An advantage of this technique is that it allows to obtain good samples when the pump flux is kept low. However, depending on the frit and the applied sampling flux, the efficiency of this technique can be strongly variable. Therefore laboratory tests should be performed in order to ensure good sampling efficiency in the field. The use of pure NaOH solution coupled with a cautious sample pretreatment provides an easy and relatively fast quantification of all species of interest and moreover it is possible to estimate the amount of dissolved volcanic CO_2.
- Raschig Tubes (BRT and SRT) were found to be very efficient sampling techniques, allowing to apply much higher air sampling fluxes than DB, while at the same time a smaller amount of sampling solution can be used. They also need glassware and solutions to be transported in the field and require even more precaution than the DB, since the rotating system requires level mounting of the device. While set-up and handling are more demanding, Raschig Tubes allow to obtain sampled species concentrations in the solution, which are one order of magnitude higher than in the DB and therefore more accurate detection of less abundant species is possible.

Within the framework of three campaigns to the Italian volcanoes Stromboli and Mt Etna, the sulfur to halogen ratios obtained by BRT, SRT, and DB are in good agreement except for deviations of the S/Br ratios, which could not properly be explained yet. Moreover, the FP results obtained in this work are consistent with the results by BRT, SRT, and DB when high plume concentrations were present and the results could be considered as significant, as declared above. Figure 15 summarizes and compares all measurement results in a ternary diagram including S, Cl and Br. As pointed out in section 5, the good accordance for the NEC results can be seen representing the good sampling

conditions and thus high analyte concentrations. Deviations are mainly noticeable for the BN and Stromboli samples and might be caused by the more challenging sampling conditions implicating low volcanogenic analyte concentrations.

At Mt Etna especially iodine shows systematic deviations between the measurement techniques. Our filter pack measurements roughly confirm the mean S/I ratio of $2.5 \cdot 10^5$ for Etna's North-East crater [*Aiuppa et al.*, 2005a] who used the same technique (FP). However, measurements with DB, BRT and SRT resulted in a range of $(4.6 – 8.2) \cdot 10^4$ indicating much higher iodine emission than initially expected. This issue has to be further investigated in the future. At Stromboli, iodine was determined for the first time and S/I ratios of $7.6 \cdot 10^4$ (SRT) and $28.4 \cdot 10^4$ (DB) were obtained.

Finally, direct sampling data were compared and combined with BrO/SO_2 ratios, simultaneously detected by MAX-DOAS measurements and provide a new data set to constrain the amount of BrO on the total emitted bromine in different plume ages.

Acknowledgments:

Special thanks to the INGV Palermo for the financial and logistical support. We also thank for financial support from the DFG project DFG3611/1-1. We are grateful to L. Brusca and S. Bellomo for the ICP-MS analysis, to H. Zeller, S. Spiegel, and R. Stadler for the technical support, to all participants of the field campaigns. We also thank the Editor and the Reviewers Franco Tassi and Bruce Christenson for the constructive comments.

References

Aiuppa, A. (2009), Degassing of halogens from basaltic volcanism: Insights from volcanic gas observations, *Chem. Geol.,* 263(1), 99–109, doi:10.1016/j.chemgeo.2008.08.022.

Aiuppa, A. and C. Federico (2004), Anomalous magmatic degassing prior to the 5th April 2003 paroxysm on Stromboli, *Geophys. Res. Lett.,* 31(14), doi:10.1029/2004GL020458.

Aiuppa, A., C. Federico, A. Paonita, G. Pecoraino, M. Valenza (2002), S, Cl and F degassing as an indicator of volcanic dynamics: The 2001 eruption of Mount Etna, *Geophys. Res. Lett.,* 29(11), doi:10.1029/2002GL015032.

Aiuppa, A., C. Federico, G. Giudice, S. Gurrieri, A. Paonita, M. Valenza (2004), Plume chemistry provides insights into mechanisms of sulfur and halogen degassing in basaltic volcanoes, *Earth and Planetary Science Letters,* 222(2), 469–483, doi:10.1016/j.epsl.2004.03.020.

Aiuppa, A., C. Federico, A. Franco, G. Giudice, S. Gurrieri, S. Inguaggiato, M. Liuzzo, A. J. S. McGonigle, M. Valenza (2005a), Emission of bromine and iodine from Mount Etna volcano, *Geochem. Geophys. Geosyst.,* 6(8), doi:10.1029/2005GC000965.

Aiuppa, A., S. Inguaggiato, A. J. S. McGonigle, M. O'Dwyer, C. Oppenheimer, M. J. Padgett, D. Rouwet, M. Valenza, A. McGonigle, M. O'Dwyer, M. Padgett (2005b), H_2S fluxes from Mt. Etna, Stromboli, and Vulcano (Italy) and implications for the sulfur budget at volcanoes, *Geochim. Cosmochim. Acta,* 69(7), 1861–1871, doi:10.1016/j.gca.2004.09.018.

Aiuppa, A., A. Bertagnini, N. Métrich, R. Moretti, A. Di Muro, M. Liuzzo, G. Tamburello (2010), A model of degassing for Stromboli volcano, *Earth Planet. Sci. Lett.,* 295(1), 195–204, doi:10.1016/j.epsl.2010.03.040.

Allard, P., J. Carbonnelle, N. Metrich, H. Loyer, P. Zettwoog (1994), Sulphur output and magma degassing budget of Stromboli volcano, *Nature,* 368(6469), 326–330, doi:10.1038/368326a0.

Allard, P., A. Aiuppa, H. Loyer, F. Carrot, A. Gaudry, G. Pinte, A. Michel, G. Dongarrà (2000), Acid Gas and Metal Emission Rates during Long-lived Basalt Degassing at Stromboli Volcano, *Geophys. Res. Lett.,* 27(8), S. 1207–1210, doi:10.1029/1999GL008413.

Anlauf, K. G., P. Fellin, H. A. Wiebe, H. I. Schiff, G. I. Mackay, R. S. Braman, R. Gilbert (1985), A comparison of three methods for measurement of atmospheric nitric acid and aerosol nitrate and ammonium, *Atmos. Environ.,* 19(2), 325–333, doi:10.1016/0004-6981(85)90100-3.

Beckman, J. S., T. W. Beckman, J. Chen, P. A. Marshall, B. A. Freeman (1990), Apparent hydroxyl radical production by peroxynitrite: implications for endothelial injury from nitric oxide and superoxide, *Proc. Nat. Acad. Sci.,* 87(4), 1620–1624, doi:10.1073/pnas.87.4.1620.

Bobrowski, N. and U. Platt (2007), SO_2/BrO ratios studied in five volcanic plumes, *J. Volcanol. Geoth. Res.,* 166(3), 147–160, doi:10.1016/j.jvolgeores.2007.07.003.

Bobrowski, N., G. Hönninger, B. Galle, U. Platt (2003), Detection of bromine monoxide in a volcanic plume, *Nature,* 423(6937), 273–276, doi:10.1038/nature01625.

Bobrowski, N., R. von Glasow, A. Aiuppa, S. Inguaggiato, I. Louban, O. W. Ibrahim, U. Platt (2007), Reactive halogen chemistry in volcanic plumes, *J. Geophys. Res.,* 112(D6), doi:10.1029/2006JD007206.

Bowyer, P. and D. Woolf (2004), Gas Exchange and Bubble-Induced Supersaturation in a Wind-Wave Tank, *J. Atmos. Oceanic Technol.,* 21(12), 1925–1935, doi:10.1175/JTECH-1666.1.

Burton, M. R., P. Allard, F. Murè, C. Oppenheimer (2003), FTIR remote sensing of fractional magma degassing at Mount Etna, Sicily, *Geol. Soc. Spec. Publ.,* 213, 281–293, doi:10.1144/GSL.SP.2003.213.01.17.

Burton, M. R., P. Allard, F. Murè, A. La Spina (2007), Magmatic Gas Composition Reveals the Source Depth of Slug-Driven Strombolian Explosive Activity, *Science,* 317(5835), 227–230, doi:10.1126/science.1141900.

Burton, M. R., T. Caltabiano, F. Murè, G. Salerno, D. Randazzo (2009), SO_2 flux from Stromboli during the 2007 eruption: Results from the FLAME network and traverse measurements, *J. Volcanol. Geoth. Res.,* 182(3), 214–220, doi:10.1016/j.jvolgeores.2008.11.025.

Calabrese, S., A. Aiuppa, P. Allard, E. Bagnato, S. Bellomo, L. Brusca, W. D'Alessandro, F. Parello (2011), Atmospheric sources and sinks of volcanogenic elements in a basaltic volcano (Etna, Italy), *Geochimica et Cosmochimica Acta,* 75(23), 7401–7425, doi:10.1016/j.gca.2011.09.040.

Calvert, S. and W. Workman (1961), The Efficiency of Small Gas Absorbers, *Am. Ind. Hyg. Assoc. J.,* 22(4), 318–324, doi:10.1080/00028896109343415.

Chiodini, G., F. Frondini, B. Raco (1996), Diffuse emission of CO2 from the Fossa crater, Vulcano Island (Italy), *Bull. Volcanol.,* 58(1), 41-50, doi:10.1007/s004450050124.

Danckwerts, P. V. (1970), Gas-liquid reactions, *McGraw-Hill*, New York.

Delmelle, P., M. Lambert, Y. Dufrêne, P. Gerin, N. Óskarsson (2007), Gas/aerosol–ash interaction in volcanic plumes: New insights from surface analyses of fine ash particles, *Earth Planet. Sci. Lett.,* 259(1), 159–170, doi:10.1016/j.epsl.2007.04.052.

Finnegan, D. L., J. P. Kotra, D. M. Hermann, W. H. Zoller (1989), The use of7LiOH-impregnated filters for the collection of acidic gases and analysis by instrumental neutron activation analysis, *Bull. Volcanol.,* 51(2), 83–87, doi:10.1007/BF01081977.

Gage, J. C. (1960), The efficiency of absorbers in industrial hygiene air analysis, *Analyst,* 85(1008), 196–203, doi:10.1039/AN9608500196.

Gerlach, T. M. (2004), Volcanic sources of tropospheric ozone-depleting trace gases, *Geochem. Geophys. Geosyst.,* 5(9), doi:10.1029/2004GC000747.

Gerlach, T. M. and B. E. Nordlie (1975), The COHS gaseous system; Part II, Temperature, atomic composition, and molecular equilibria in volcanic gases, *Am. J. Sci.,* 275(4), 377–394, doi:10.2475/ajs.275.4.377.

Giggenbach, W. F. (1975), A Simple Method for the Collection and Analysis of Volcanic Gas Samples, *Bull. Volcanol.,* 39(1), 132–145, doi:10.1007/BF02596953.

Giggenbach, W. F. and S. Matsuo (1991), Evaluation of results from Second and Third IAVCEI Field Workshops on Volcanic Gases, Mt Usu, Japan, and White Island, New Zealand, *Appl Geochem.,* 6(2), 125–141, doi:10.1016/0883-2927(91)90024-J.

Glasow, R. von (2010), Atmospheric chemistry in volcanic plumes, *Proc. Nat. Acad. Sci.,* 107(15), 6594–6599, doi:10.1073/pnas.0913164107.

Glasow, R. von, N. Bobrowski, C. Kern (2009), The effects of volcanic eruptions on atmospheric chemistry, *Chem. Geol.,* 263(1),131–142, doi:10.1016/j.chemgeo.2008.08.020.

Hoffmann, M. R. (1977), Kinetics and mechanism of oxidation of hydrogen sulfide by hydrogen peroxide in acidic solution, Environ. Sci. Technol., 11(1), S. 61–66, doi:10.1021/es60124a004.Honda, F. (1970), Geochemical study of iodine in volcanic gases. II. Behaviour of iodine in volcanic gases, *Geochem. J,* 3, 201–211.

Honda, F., Y. Mizutani, T. Sugiura, S. Oana (1966), A Geochemical Study of Iodine in Volcanic Gases, *Bull. Chem. Soc. Jpn.,* 39(12), S. 2690-2695, doi:10.1246/bcsj.39.2690.

Huygen, C. (1962), The Sampling of Sulfur Dioxide in air with impregnated filter paper, *Anal. Chim. Acta,* 28, 349–360, doi:10.1016/S0003-2670(00)87244-X.

Huygen, C. (1963), The Sampling of Hydrogen Fluoride in air with impregnated filter paper, *Anal. Chim. Acta,* 29, 448–452, doi:10.1016/S0003-2670(00)88644-4.

Jagger, T. A. (1940), Magmatic gases, *Am. J. Sci.*(238), S. 313–353, doi:10.2475/ajs.238.5.313.

Jähne, B. and H. Haußecker (1998), Air-Water Gas Exchange, *Annu. Rev. Fluid Mech.,* 30(1), 443–468, doi:10.1146/annurev.fluid.30.1.443.

Kerth, J. and D. Jensen (1995), Determinations of trace anions in hydrogen peroxide, *J. Chromatogr.*, 706(1–2), S. 191–198, doi:10.1016/0021-9673(94)01277-L.

La Spina, A., M. R. Burton, G. G. Salerno (2010), Untravelling the processes controlling gas emissions from the central and northeast craters of Mt. Etna, *J. Volcanol. Geoth. Res.,* 198(3), 368–376, doi:10.1016/j.jvolgeores.2010.09.018.

La Spina, A., M. Burton, R. Harig, F. Mure, P. Rusch, M. Jordan, T. Caltabiano (2013), New insights into volcanic processes at Stromboli from Cerberus, a remote-controlled open-path FTIR scanner system, *J. Volcanol. Geoth. Res.,* 249, 66–76, doi:10.1016/j.jvolgeores.2012.09.004.

Levin, I. (1978), Regionale Modellierung des atmosphärischen CO_2 aufgrund von C-13-und C-14-messungen, PhD thesis, Inst. for Environ. Phys., *Univ. of Heidelberg, Heidelberg, Germany*.

Levin, I. and W. Weiss (1980), The effect of anthropogenic CO_2 and $_{14}C$ sources on the distribution of $_{14}C$ in the atmosphere, *Radiocarbon,* 22(2), 379–381.

Liotta, M., L. Brusca, F. Grassa, S. Inguaggiato, M. Longo, P. Madonia (2006), Geochemistry of rainfall at Stromboli volcano (Aeolian Islands): Isotopic composition and plume-rain interaction, *Geochem. Geophys. Geosyst.,* 7(7), doi:10.1029/2006GC001288.

Liotta, M., A. Paonita, A. Caracausi, M. Martelli, A. Rizzo, R. Favara (2010), Hydrothermal processes governing the geochemistry of the crater fumaroles at Mount Etna volcano (Italy), *Chem. Geol.,* 278(1), 92–104, doi:10.1016/j.chemgeo.2010.09.004.

Liotta, M., A. Rizzo, A. Paonita, A. Caracausi, M. Martelli (2012), Sulfur isotopic compositions of fumarolic and plume gases at Mount Etna (Italy) and inferences on their magmatic source, *Geochem. Geophys. Geosyst.,* 13(5), doi:10.1029/2012GC004118.

Maaß, F., H. Elias, K. J. Wannowius (1999), Kinetics of the oxidation of hydrogen sulfite by hydrogen peroxide in aqueous solution:: ionic strength effects and temperature dependence, *Atmos. Environ.,* 33(27), 4413–4419, doi:10.1016/S1352-2310(99)00212-5.

Martin, R. S., T. A. Mather, D. M. Pyle, M. Power, A. G. Allen, A. Aiuppa, C. J. Horwell, E. P. Ward (2008), Composition- resolved size distributions of volcanic aerosols in the Mt. Etna plumes, *J. Geophys. Res.,* 113(D17), doi:10.1029/2007JD009648.

Mather, T. A. and D. M. Pyle (2008), Investigation of the use of filter packs to measure the sulphur isotopic composition of volcanic sulphur dioxide and the sulphur and oxygen isotopic composition of volcanic sulphate aerosol, *Atmos. Environ.,* 42(19), 4611–4618, doi:10.1016/j.atmosenv.2008.01.052.

Mather, T. A., C. Oppenheimer, A. G. Allen, A. J. S. McGonigle (2004), Aerosol chemistry of emissions from three contrasting volcanoes in Italy, *Atmos. Environ.,* 38(33), 5637–5649, doi:10.1016/j.atmosenv.2004.06.017.

McGonigle, A. J. and C. Oppenheimer (2003), Optical sensing of volcanic gas and aerosol emissions, *Geological Society, London, Special Publications,* 213(1), 149–168, doi:10.1144/GSL.SP.2003.213.01.09.

Mioduszewski, L. and V. Kress (2008), Laboratory calibration of chemical volcanic gas sampling techniques using an artificial fumarole, *J. Volcanol. Geoth. Res.,* 174(4), 295–306, doi:10.1016/j.jvolgeores.2008.02.006.

Montegrossi, G., F. Tassi, O. Vaselli, A. Buccianti, K. Garofalo (2001), Sulfur Species in Volcanic Gases, *Anal. Chem.,* 73(15), S. 3709–3715, doi:10.1021/ac001429b.

Mori, T. and M. Burton (2009), Quantification of the gas mass emitted during single explosions on Stromboli with the SO_2 imaging camera, *J. Volcanol. Geoth. Res.,* 188(4), 395–400, doi:10.1016/j.jvolgeores.2009.10.005.

Novic, M., B. Lecnik, V. Hudnik, B. Pihlar (1997), Carbonate interference by ion chromatographic determination of anions in mineral waters, *J. Chromatogr.,* 764(2), 249–256, doi:10.1016/S0021-9673(96)00905-3.

Oppenheimer, C., V. I. Tsanev, C. F. Braban, R. A. Cox, J. W. Adams, A. Aiuppa, N. Bobrowski, P. Delmelle, J. Barclay, A. J. S. McGonigle (2006), BrO formation in volcanic plumes, *Geochim. Cosmochim. Acta,* 70(12), 2935–2941, doi:10.1016/j.gca.2006.04.001.

Pennisi, M. and M. F. Le Cloarec (1998), Variations of Cl, F, and S in Mount Etna's plume, Italy, between 1992 and 1995, *J. Geophys. Res.,* 103(B3), 5061–5066, doi:10.1029/97JB03011.

Platt, U. and J. Stutz (2008), Differential absorption spectroscopy, *Springer*, Berlin.

Rizzo, A. L., A. Caracausi, M. Liotta, A. Paonita, J. D. Barnes, R. A. Corsaro, M. Martelli (2013), Chlorine isotope composition of volcanic gases and rocks at Mount Etna (Italy) and inferences on the local mantle source, *Earth Planet. Sci. Lett.,* 371–372(0), 134–142, doi:10.1016/j.epsl.2013.04.004.

Roberts, L. R. and H. C. Mckee (1959), Evaluation of Absorption Sampling Devices, *Journal of the Air Pollution Control Association,* 9(1), 51–53, doi:10.1080/00022470.1959.10467873.

Roberts, T. J., C. F. Braban, R. S. Martin, C. Oppenheimer, J. W. Adams, R. A. Cox, R. L. Jones, P. T. Griffiths (2009), Modelling reactive halogen formation and ozone depletion in volcanic plumes, *Chem. Geol.,* 263(1), 151–163, doi:10.1016/j.chemgeo.2008.11.012.

Roghair, I., Y. M. Lau, N. G. Deen, H. M. Slagter, M. W. Baltussen, M. van Sint Annaland, J. A. M. Kuipers (2011), On the drag force of bubbles in bubble swarms at intermediate and high Reynolds numbers, *10th International Conference on Gas–Liquid and Gas–Liquid–Solid Reactor Engineering,* 66(14), 3204–3211, doi:10.1016/j.ces.2011.02.030.

Rose, W. I. (1977), Scavenging of volcanic aerosol by ash: Atmospheric and volcanologic implications, *Geology,* 5(10), S. 621–624, doi:10.1130/0091-7613(1977)5<621:SOVABA>2.0.CO;2.

Sander, R. (1999), Compilation of Henry's law constants for inorganic and organic species of potential importance in environmental chemistry, *Max-Planck Institute of Chemistry, Air Chemistry Department*. doi: http://www.mpch-mainz.mpg.de/.

Sedlacek, W. A., A. L. Lazrus, B. W. Gandrud (1984), Measurements of stratospheric bromine, *J. Geophys. Res.,* 89(D3), S. 4821–4825, doi:10.1029/JD089iD03p04821.

Seinfeld, J. H. and S. N. Pandis (1998), Atmospheric Chemistry and Physics, From Air Pollution to Climate Change, *John Wiley and Sons Ltd.*, New York.

Shinohara, H., A. Aiuppa, G. Giudice, S. Gurrieri, M. Liuzzo (2008), Variation of H_2O/CO_2 and CO_2/SO_2 ratios of volcanic gases discharged by continuous degassing of Mount Etna volcano, Italy, *J. Geophys. Res.,* 113(B9), doi:10.1029/2007JB005185.

Siegenthaler, U. and K. O. Muennich (1981), $^{13}C/^{12}C$ fractionation during CO_2 transfer from air to sea, SCOPE 16 : Carbon Cycle Modeling (ed: B. Bolin), 246-257, *John Wiley and Sons Ltd.*, New York.

Simonnet, M., C. Gentric, E. Olmos, N. Midoux (2007), Experimental determination of the drag coefficient in a swarm of bubbles, *Chem. Eng. Sci.,* 62(3), 858–866, doi:10.1016/j.ces.2006.10.012.

Snyder, G. T. and U. Fehn (2002), Origin of iodine in volcanic fluids: 129I results from the Central American Volcanic Arc, *Geochim. Cosmochim. Acta,* 66(21), 3827–3838, doi:10.1016/S0016-7037(02)00825-6.

Sparks, R. S. (2003), Dynamics of magma degassing, *Geol. Soc. Spec. Publ.,* 213(1), 5–22, doi:10.1144/GSL.SP.2003.213.01.02.

Spilliaert, N., N. Métrich, P. Allard (2006), S–Cl–F degassing pattern of water-rich alkali basalt: Modelling and relationship with eruption styles on Mount Etna volcano, *Earth Planet. Sci. Lett.,* 248(3–4), 772–786, doi:10.1016/j.epsl.2006.06.031.

Stoiber, R. E., S. N. Williams, B. J. Huebert (1986), Sulfur and halogen gases at Masaya caldera complex, Nicaragua: total flux and variations with time, *J. Geophys. Res.,* 91(B12), 12215–12231, doi:10.1029/JB091iB12p12215.

Symonds, R. B., W. I. Rose, G. J. S. Bluth, T. M. Gerlach (1994), Volcanic-gas studies; methods, results, and applications, *Rev. Mineral Geochem.,* 30(1), 1–66.

Tedesco, D. and J.-P. Toutain (1991), Chemistry and emission rate of volatiles from White Island Volcano (New Zealand), *Geophys. Res. Lett.,* 18(1), 113–116, doi:10.1029/90GL01477.

Toutain, J. P., F. Sortino, B. Reynier, B. Dupre, M. Munoz, A. Nonell, M. Polve, S. Chancha Do Vale (2003), A new collector for sampling volcanic aerosols, *J. Volcanol. Geoth. Res.,* 123(1), 95–103, doi:10.1016/S0377-0273(03)00030-1.

Witham, C. S., C. Oppenheimer, C. J. Horwell (2005), Volcanic ash-leachates: A review and recommendations for sampling methods, *J. Volcanol. Geoth. Res.,* 141(3), 299–326, doi:10.1016/j.jvolgeores.2004.11.010.

Witt, M. L., T. A. Mather, D. M. Pyle, A. Aiuppa, E. Bagnato, V. I. Tsanev (2008), Mercury and halogen emissions from Masaya and Telica volcanoes, Nicaragua, *J. Geophys. Res.,* 113(B6), doi:10.1029/2007JB005401.

Witter, J. B. and P. Delmelle (2004), Acid gas hazards in the crater of Villarrica volcano (Chile), *Rev. Geol. Chile,* 31(2), 273–277, doi:10.4067/S0716-02082004000200006.

Witter, J. B., V. C. Kress, P. Delmelle, J. Stix (2004), Volatile degassing, petrology, and magma dynamics of the Villarrica Lava Lake, Southern Chile, *J. Volcanol. Geoth. Res.,* 134(4), 303–337, doi:10.1016/j.jvolgeores.2004.03.002.

Tables

Table 1. Weather conditions during Stromboli and Etna campaigns obtained by a portable weather station (mean values over sampling time).

Date	Relative humidity (%)	Temperature (°C)	Atmospheric pressure (hPa)	Sky cover	Wind speed (m/s)	Plume age (min)
Stromboli						
29.09.11	54	23	912	No clouds	< 1	4 - 8
19.06.12	30	27	926	No clouds	1.1	≈ 3
20.06.12	28	27	919	No clouds	2.5	≈ 1.4
21.06.12	21	29	920	No clouds	1.1	≈ 2.6
Etna						
26.06.12	57	15	685	No clouds	4.2	< 1
27.06.12	66	13	690	Light clouds	2.4	< 1

Table 2. Sample data for the measurements at Stromboli (STR) and the craters of Mount Etna (North-East Crater and Bocca Nuova – NEC and BN respectively) and the resulting molar analyte concentrations.

Date	Sample Name	Instrument	Filter number	Flow (l/min)	Sampled air volume (l) ± 5%	Sulfur [mmol/l]	Chlorine [mmol/l]	Fluorine [mmol/l]	Bromine [µmol/l]	Iodine [nmol/l]
28.09.11	Atmospheric Blank	DB		1	155	0.006 ± 0.001	0.002 ± 0.002	-	0.018 ± 0.003	4.68 ± 0.54
29.09.11	STR 0.1	DB		0.94	175	0.006 ± 0.001	0.002 ± 0.002	-	0.023 ± 0.003	2.18 ± 0.07
	STR 0.2	DB		0.94	174	0.033 ± 0.001	0.018 ± 0.002	-	0.039 ± 0.003	2.13 ± 0.09
19.06.12	STR 1.1	BRT		4	401	0.005 ± 0.001	0.017 ± 0.002	-	0.118 ± 0.006	18.57 ± 1.41
	STR 1.2	SRT		4	400	0.016 ± 0.001	0.070 ± 0.003	-	0.082 ± 0.005	9.18 ± 0.17
20.06.12	STR 2.1	DB		2	331	0.18 ± 0.01	0.12 ± 0.002	0.0128 ± 0.0004	0.231 ± 0.004	13.48 ± 0.52
	STR 2.2	SRT		4	382	0.83 ± 0.04	0.52 ± 0.01	0.051 ± 0.002	0.650 ± 0.020	14.22 ± 1.35
	STR 2.3	FP	A	4	101	0.93 ± 0.04	0.87 ± 0.01	-	0.797 ± 0.003	11.65 ± 0.25
			B			0.06 ± 0.005	-	-	0.054 ± 0.005	0.39 ± 0.12
			C			0.005 ± 0.001	0.012 ± 0.001	-	0.038 ± 0.003	0.86 ± 0.22
	STR 2.4	FP	A	4	116	0.35 ± 0.015	0.31 ± 0.03	-	0.327 ± 0.004	3.04 ± 0.10
			B			0.005 ± 0.001	-	-	0.011 ± 0.001	-
			C			0.005 ± 0.001	-	-	0.013 ± 0.001	0.65 ± 0.06
	STR 2.5	FP	A	5	130	0.87 ± 0.04	0.69 ± 0.01	-	0.687 ± 0.016	13.44 ± 0.43
			B			0.065 ± 0.005	0.010 ± 0.001	-	0.028 ± 0.001	-
			C			0.005 ± 0.001	-	-	0.028 ± 0.004	0.33 ± 0.14
21.06.12	STR 3.1	DB		1	101	0.088 ± 0.004	0.060 ± 0.002	0.0069 ± 0.0004	0.150 ± 0.002	16.12 ± 0.32
	STR 3.2	SRT		5	535	1.17 ± 0.05	0.798 ± 0.007	0.064 ± 0.002	0.852 ± 0.014	12.43 ± 0.27
	STR 3.3	FP	A	1	103	0.92 ± 0.04	1.20 ± 0.01	-	0.93 ± 0.01	9.76 ± 0.31
			B			0.01 ± 0.001	-	-	0.028 ± 0.002	-
			C			0.005 ± 0.001	-	-	0.023 ± 0.001	-
	STR 3.4	FP	A	5	68	0.4 ± 0.02	0.33 ± 0.003	-	0.32 ± 0.02	2.67 ± 0.33
			B			0.01 ± 0.001	0.009 ± 0.003	-	0.018 ± 0.001	0.32 ± 0.08
			C			0.01 ± 0.001	0.010 ± 0.001	-	0.021 ± 0.001	-
26.06.12	NEC 1.1	DB		2	178	0.48 ± 0.02	0.25 ± 0.003	0.050 ± 0.001	0.500 ± 0.015	11.33 ± 0.57
	NEC 1.2	SRT		4	361	3.14 ± 0.14	1.70 ± 0.02	0.579 ± 0.017	2.69 ± 0.03	38.34 ± 0.33
	NEC 1.3	BRT		4	363	1.43 ± 0.06	0.78 ± 0.01	0.261 ± 0.007	1.19 ± 0.03	24.87 ± 0.37
	NEC 1.4	FP	A	4	21	0.57 ± 0.03	0.35 ± 0.003	-	0.536 ± 0.008	6.32 ± 0.08
			B			0.005 ± 0.001	0.015 ± 0.001	-	0.019 ± 0.002	-
			C			0.005 ± 0.001	0.012 ± 0.001	-	0.013 ± 0.001	1.43 ± 0.07
	NEC 1.5	FP	A	4	20	0.75 ± 0.04	0.46 ± 0.01	-	0.723 ± 0.010	8.16 ± 0.15
			B			0.015 ± 0.001	0.010 ± 0.001	-	0.016 ± 0.001	-
			C			0.003 ± 0.001	0.010 ± 0.001	-	0.009 ± 0.002	-
30.09.11	NEC 2.1[a, b]	FP	A	5	220	0.54	1.42	0.36		
			B			0.53	0.07	0.02		
			C			0.45	0.11	0.02		
	NEC 2.2[a, b]	FP	A	5	220	0.37	1.60	0.44		
			B			0.52	-	0.023		
			C			0.49	-	0.003		
04.08.11	NEC 3	DB		0.83	68	0.44 ± 0.01	0.22 ± 0.002	0.090 ± 0.003	0.401 ± 0.005	9.13 ± 0.09
02.07.11	NEC 4.1[a, b]	FP	A	5	153	0.36	2.78	0.76		
			B			0.47	0.73	0.48		
			C			0.83	-	0.02		
	NEC 4.2[a, b]	FP	A	5	153	0.53	2.83	1.07		
			B			0.77	0.31	0.14		
			C			0.84	0.68	0.21		

Date	Sample Name	Instrument	Filter number	Flow (l/min)	Sampled air volume (l) ± 5%	Sulfur [mmol/l]	Chlorine [mmol/l]	Fluorine [mmol/l]	Bromine [µmol/l]	Iodine [nmol/l]
04.07.11	NEC 4.3	DB		0.83	89	0.95 ± 0.03	0.54 ± 0.004	0.147 ± 0.005	0.951 ± 0.01	20.07 ± 0.28
	NEC 4.4[a, b]	FP	A	5	153	1.23	6.95	1.27		
			B			4.80	0.97	1.27		
			C			3.86	1.62	0.21		
	NEC 4.5[a, b]	FP	A	5	153	1.10	8.10	1.32		
			B			2.86	1.18	1.63		
			C			4.72	0.24	0.02		
24.06.11	NEC 5[a]	FP	A	5	155	1.52	0.83	0.278	1.354	24.78
			B			0.08	-	0.002	0.069	3.90
			C			0.05	-	0.002	0.016	0.37
27.06.12	BN 1.1	DB		2	126	0.32 ± 0.01	0.072 ± 0.002	0.0053 ± 0.0004	0.181 ± 0.003	4.07 ± 0.17
	BN 1.2	SRT		5	172	0.84 ± 0.04	0.321 ± 0.004	0.0036 ± 0.0002	0.436 ± 0.041	6.38 ± 1.19
	BN 1.3	BRT		4	299	0.53 ± 0.02	0.164 ± 0.003	-	0.238 ± 0.020	13.48 ± 0.20
	BN 1.4	FP	A	4	125	1.18 ± 0.05	0.36 ± 0.003	-	0.415 ± 0.002	6.1 ± 0.16
			B			0.23 ± 0.01	0.089 ± 0.005	-	0.053 ± 0.001	0.27 ± 0.07
			C			0.08 ± 0.01	0.013 ± 0.001	-	0.026 ± 0.004	-
30.09.11	BN 2.1	DB		0.83	136	0.57 ± 0.02	0.181 ± 0.002	-	0.250 ± 0.006	7.88 ± 0.20
	BN 2.2[a, b]	FP	A	5	150	1.05	2.68	0.089		
			B			1.54	0.13	0.004		
			C			1.15	0.10	0.002		
	BN 2.3[a, b]	FP	A	5	150	0.90	2.61	0.089		
			B			1.12	-	0.01		
			C			1.05	0.09	0.03		
24.06.11	BN 3	FP	A			1.28	0.49	0.029	0.620	20.79
			B			0.68	-	0.007	0.138	7.57
			C			0.06	-	0.002	0.024	1.82
20.10.10	BN 4.1	DB		0.83	62	0.74 ± 0.02	0.210 ± 0.002	-	0.360 ± 0.007	29.51 ± 0.97
	BN 4.2[a, b]	FP	A	4	172	1.99	3.79	0.11		
			B			2.27	0.19	0.01		
			C			1.72	0.06	0.004		
	BN 4.3[a, b]	FP	A	4	172	2.20	3.70	0.1		
			B			2.48	0.23	0.007		
			C			1.40	0.07	0.004		
10.08.10	BN 5.1[a]	FP	A	4	128	1.80	0.82	0.10	0.663	12.05
			B			1.15	0.27	0.03	0.470	9.93
			C			0.23	0.34	0.03	0.083	3.30
	BN 5.2[a]		A	4	128	5.03	3.59	0.33	2.242	48.39
			B			4.19	0.29	0.07	0.278	9.55
			C			0.46	-	0.03	0.119	2.65
24.06.10	BN 5.1	DB		0.83	174	0.65 ± 0.02	0.222 ± 0.002	0.0081 ± 0.0005	0.339 ± 0.003	18.82 ± 0.30
	BN 5.2[a, b]	FP	A	4	720	4.46	4.85	2.73		
			B			6.67	1.22	0.23		
			C			5.34	0.20	0.36		
	Blank 1 (FP)					0.001 ± 0.0002	0.013 ± 0.001	-	0.032 ± 0.001	0.69 ± 0.12
	Blank 2 (FP)					0.002 ± 0.0003	0.010 ± 0.001	-	0.019 ± 0.002	-
	Blank 3 (FP)					0.003 ± 0.0004	0.011 ± 0.001	-	-	-
	1 M NaOH					0.0017 ± 0.0003	0.0038 ±	-	-	2.7 ± 0.15
	1.5 M NaOH					0.0011 ± 0.0002	-	-	-	3.4 ± 0.14

[a]Samples were analyzed in various IC, ICP-MS analytical sessions. The uncertainty can be estimated to <10 %. Results for fluoride were obtained by an ion selective electrode.
[b]Samples containing 10% or more of the total element concentration in the 3rd stage are deleted from discussion

Table 3. Typical concentrations of the detected volcanic elements in the air (mean over RT and DB) at the sampling sites (atmospheric background subtracted) for the different dates calculated based on the molar concentrations and the sampled air volume.

Location (Number of samples)	Date	CO_2 (ppm)	S (ppm)	Cl (ppm)	F (ppm)	Br (ppb)
Etna-NEC (1)	04.07.2011	120 ± 73	36.4 ± 1.8	20.6 ± 0.2	5.65 ± 0.19	36.5 ± 0.37
Etna-NEC (1)	04.08.2011	180 ± 81	21.9 ± 0.7	11.1 ± 0.1	4.52 ± 0.15	20.1 ± 0.25
Etna-NEC (3)	26.06.2012	74 ± 28	11.5 ± 2.1	6.14 ± 1.3	1.86 ± 0.73	10.3 ± 0.24
Etna-BN (1)	24.06.2010	222 ± 69	12.4 ± 0.4	4.22 ± 0.05	0.15 ± 0.01	6.45 ± 0.05
Etna-BN (1)	20.10.2010	167 ± 80	38.5 ± 1.3	11.0 ± 0.1	0.11 ± 0.003	18.8 ± 0.37
Etna-BN (1)	30.09.2011	527 ± 104	13.9 ± 0.5	4.43 ± 0.06	0.05 ± 0.002	6.14 ± 0.14
Etna-BN (3)	27.06.2012	483 ± 77	7.84 ± 0.6	2.40 ± 0.6	0.09 ± 0.08	4.05 ± 0.78
STR (1)	29.09.2011	n.d.	0.51 ± 0.02	0.28 ± 0.03	n.d.	0.59 ± 0.04
STR (2)	19.06.2012	n.d.	0.04 ± 0.05	0.14 ± 0.01	n.d.	0.49 ± 0.40
STR (2)	20.06.2012	18 ± 2	1.39 ± 0.02	0.89 ± 0.01	0.09 ± 0.03	1.45 ± 0.49
STR (2)	21.06.2012	23 ± 30	2.46 ± 0.06	1.59 ± 0.05	0.16 ± 0.03	2.91 ± 1.50

Table 4. Molar ratios (± standard deviation) of volcanogenic elements obtained by the applied instruments for the attended sampling sites from 2010 to 2012. In the case when only one sample is present the analytical uncertainty is displayed.

Location (Number of samples)	**Instrument**	**CO_2/S**	**S/Cl**	**S/F**	**S/Br**	**S/I·10^4**
NEC (3)	DB	6.7 ± 2.9	1.89 ± 0.11	7.0 ± 2.5	1015 ± 66	4.6 ± 0.3
NEC (1)	SRT	3.6 ± 2.5	1.85 ± 0.08	5.4 ± 0.3	1167 ± 52	8.2 ± 0.4
NEC (1)	BRT	7.5 ± 2.5	1.83 ± 0.08	5.5 ± 0.3	1206 ± 63	6.5 ± 0.4
NEC (3)	FP	-	1.79 ± 0.18	5.9[a]	1123 ± 38	18 ± 12
BN (4)	DB	26.7 ± 19.1	3.5 ± 0.7	70 ± 15	2000 ± 214	5.3 ± 2.7
BN (1)	SRT	67.1 ± 7.4	2.6 ± 0.1	-	1925 ± 198	13.1 ± 2.5
BN (1)	BRT	73.1 ± 8.1	3.2 ± 0.2	-	2217 ± 212	5.0 ± 0.2
BN (4)	FP	-	3.1 ± 0.9	31 ± 19[a]	3128 ± 581	14.4 ± 7.0
STR (2)	DB	16.4 ± 3.9	1.59 ± 0.18	13.2 ± 0.7	673 ± 136	1.1 ± 0.5
STR (2)	SRT	11.8 ± 7.9	1.61 ± 0.03	17.3 ± 1.5	1279 ± 68	7.6 ± 2.5
STR (4)	FP	-	1.25 ± 0.11	-	1287 ± 119	28.4 ± 7.8

[a]Results for fluoride were obtained by an ion selective electrode – only samples from 2010 and 2011 are considered

Table 5. Br/S and BrO/SO_2 ratios obtained by direct sampling and MAX-DOAS measurements. For BrO/Br, total captured sulfur by direct sampling was equated to SO_2. R2 is a measure of the "goodness of fit" and defined as 1-sum of squared residual/total sum of squares. n.d. = not detected (not possible to detect or under detection limit).

	Direct sampling		**MAX-DOAS**			
Location/ Date	Plume age [min]	Mean Br/S ($\times 10^{-4}$)	Plume age [min]	Mean BrO/SO_2 ($\times 10^{-4}$)	R^2	BrO/Br
Stromboli						
19.06.2012		n.d.	< 1	0.57 ± 0.03	0.96	0.071 ± 0.004 [a]
20.06.2012	≈ 1	8.0 ± 0.6	≈ 4.5	0.86 ± 0.06	0.70	0.108 ± 0.008
21.06.2012	≈ 1	8.1 ± 1.5	≈ 75	0.60 ± 0.06	0.74	0.075 ± 0.008
Mt Etna						
26.06.2012 (NEC)	≈ 1	8.8 ± 0.4	< 1	0.26 ± 0.02	0.89	0.030 ± 0.002
27.06.2012 (BN)	≈ 1	4.2 ± 1.2	< 1	0.24 ± 0.02	0.75	0.057 ± 0.006

[a]The calculation is based on the mean Br/S in June 20, 2012

Figure captions

Figure 1. Scheme and dimensions of the BRT (SRT) (a), operating mode of the BRT (b) and close up view on the SRT (c). The small arrows in (b) indicate the direction of the gas flow and the blue curved arrow indicates the rotation.

Figure 2. The effect of 5 µl H_2O_2 on Milli-Q water before and after treatment with MnO_2 and sonication.

Figure 3. Extracted chloride peak of the neutralized ("untreated") NEC 2 sample (pH ≈ 4) (b) Extracted chloride peak of the neutralized NEC 2 sample with pH adjustment (pH ≈ 8). The untreated sample shows a 3.5 % smaller peak area for chloride.

Figure 4. Concentration of an element when a divalent species i is trapped in a not saturated NaOH solution as a function of sampling time and the molar air fraction in ppm for the small Raschig-Tube (45 ml NaOH, Q = 4 l/min) and the Drechsel bottle (100 ml NaOH, Q = 1 l/min). As an orientation the dashed saturation line for a 1 M NaOH solution, indicates the simplified assumption that one mole CO_2 or one mole SO_2 reacted with two mole OH^- ions. The changeover to dotted lines represents the trend for solutions with higher molarity.

Figure 5. Theoretical absorption efficiency expressed as the fraction of absorbed CO_2 for the BRT, SRT, and two DBs with different frits (different bubble radii) as a function of the pump flow. Used parameters (small Raschig-Tube in parenthesis): w = 0.34 cm/s [*Siegenthaler and Muennich,* 1981], $\alpha = 0.6$, $C_D = 2$, h = 10 cm, $\rho = 3.6$ rings/cm^3, $A_r = 2.07$ cm^2, $A_{eff} = 63.9$ (31.3) cm2, L = 13 (8) cm, DB 1: r (Q = 1 l/min) = 0.15 cm, DB 2: r (Q = 1 l/min) = 0.2 cm.

Figure 6. Molar S/Cl ratio versus sampled air volume for the Etna samples.

Figure 7. Sulfur concentration versus chlorine (blue) and bromine (green) concentration measured in the sample solutions of NEC with linear regression (forced through 0). For the FP samples the mean molar concentration of all three filters is displayed.

Figure 8. Sulfur concentration versus chlorine (blue) and bromine (green) concentration measured in the sample solutions of BN with linear regression (forced through 0). For the FP samples the mean molar concentration of all three filters is displayed.

Figure 9. Ternary diagram for Etna's NEC that compares ratios of sulfur, chlorine and fluorine for samples analyzed in this work and published values from *La Spina et al.* [2010], *Martin et al.* [2008], *Aiuppa et al.* [2009, 2005a], and *Burton et al.* [2003].

Figure 10. Ternary diagram for Etna's BN that compares ratios of sulfur, chlorine and fluorine for samples analyzed in this work and published values from *La Spina et al.* [2010], *Martin et al.* [2008], *Aiuppa et al.* [2009, 2005], and *Burton et al.* [2003].

Figure 11. Molar S/Cl ratio versus sampled air volume for the Stromboli samples.

Figure 12. Sulfur concentration versus chlorine (blue) and bromine (green) concentration measured in the sample solutions of Stromboli 2012 with linear regression (forced through 0). For the FP samples the mean molar concentration of all three filters is displayed.

Figure 13. Molar S/Br versus molar S/F ratio for Stromboli samples evaluated in this work and for ratios obtained by *Allard et al.* [2000] with filter packs for different states of activity (low, medium, high).

Figure 14. Ternary diagram that compares ratios of sulfur, chlorine and fluorine for Stromboli samples analyzed in this work and published values from *Allard et al.* [1994, 2000] and *Aiuppa and Federico* [2004].

Figure 15. Ternary diagram summarizing measurements at Etna's BN and NEC crater and Stromboli. Ratios of sulfur, chlorine and bromine are compared for samples taken by DB, SRT, BRT and FP.

Table captions

Table 1. Weather conditions during Stromboli and Etna campaigns obtained by a portable weather station (mean values over sampling time).

Table 2. Sample data for the measurements at Stromboli (STR) and the craters of Mount Etna (North-East Crater and Bocca Nuova – NEC and BN respectively) and the resulting molar analyte concentrations.

Table 3. Typical concentrations of the detected volcanic elements in the air (mean over RT and DB) at the sampling sites (atmospheric background subtracted) for the different dates calculated based on the molar concentrations and the sampled air volume.

Table 4. Molar ratios (± standard deviation) of volcanogenic elements obtained by the applied instruments for the attended sampling sites from 2010 to 2012. In the case when only one sample is present the analytical uncertainty is displayed.

Table 5. Br/S and BrO/SO_2 ratios obtained by direct sampling and MAX-DOAS measurements. For BrO/Br, total captured sulfur by direct sampling was equated to SO_2. R2 is a measure of the ”goodness of fit” and defined as 1-sum of squared residual/total sum of squares. n.d. = not detected (not possible to detect or under detection limit).

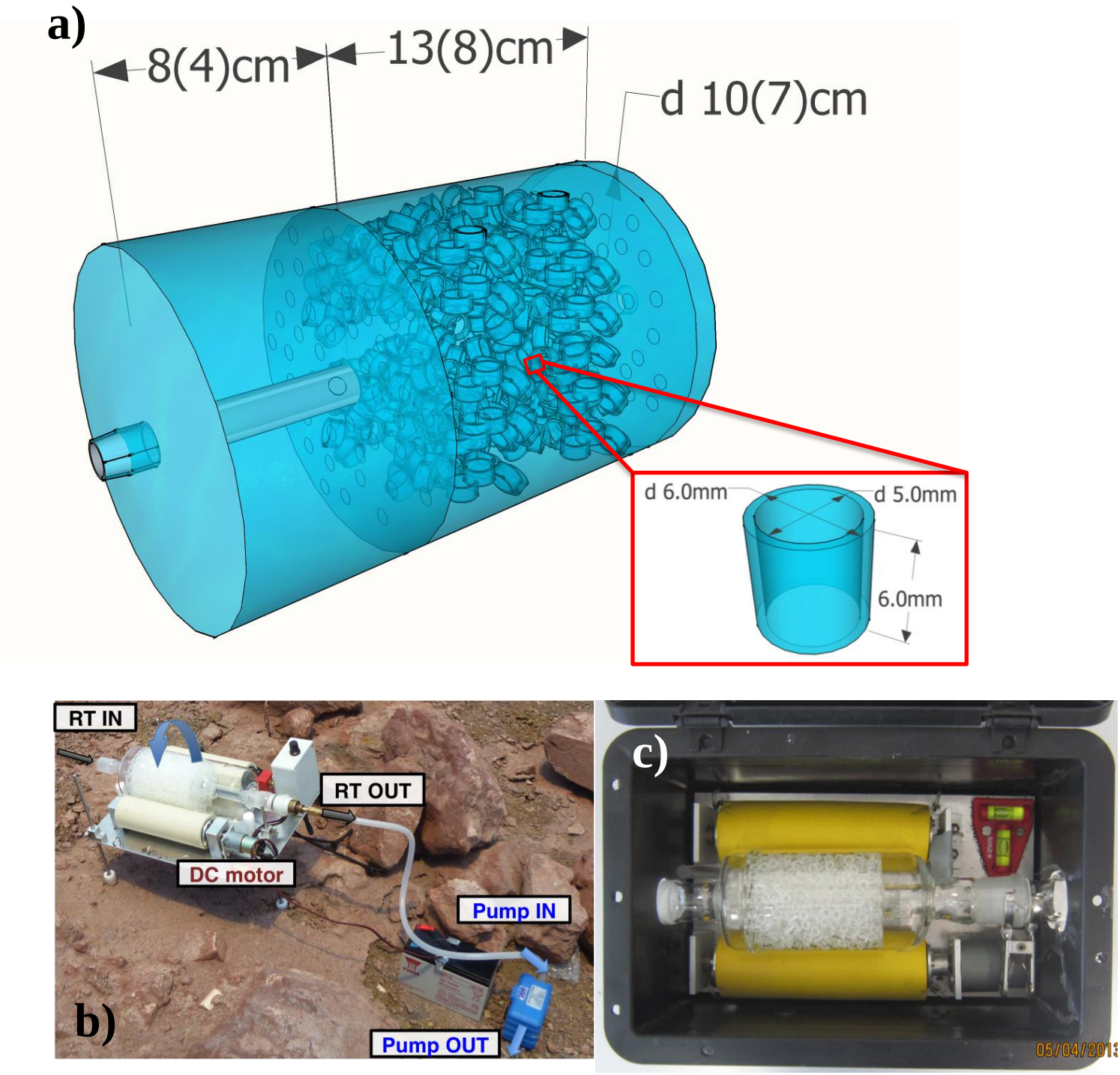
a)
8(4)cm
13(8)cm
d 10(7)cm
d 6.0mm
d 5.0mm
6.0mm
RT IN
RT OUT
DC motor
Pump IN
Pump OUT
b)
c)
05/04/2013

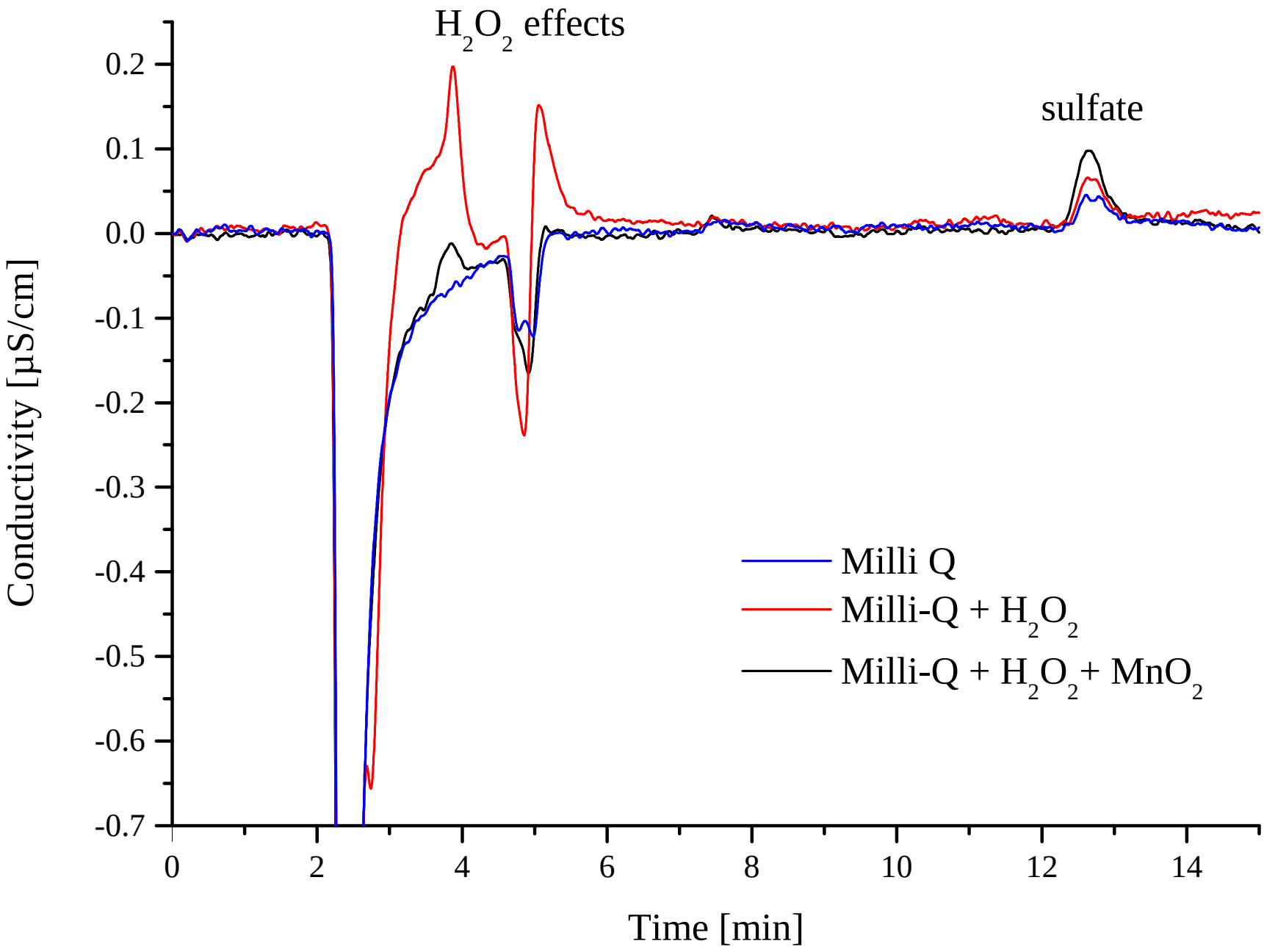
H2O2 effects
sulfate
Conductivity [µS/cm]
Time [min]
0.2
0.1
0.0
-0.1
-0.2
-0.3
-0.4
-0.5
-0.6
-0.7
0
2
4
6
8
10
12
14
Milli Q
Milli-Q + H2O2
Milli-Q + H2O2+ MnO2

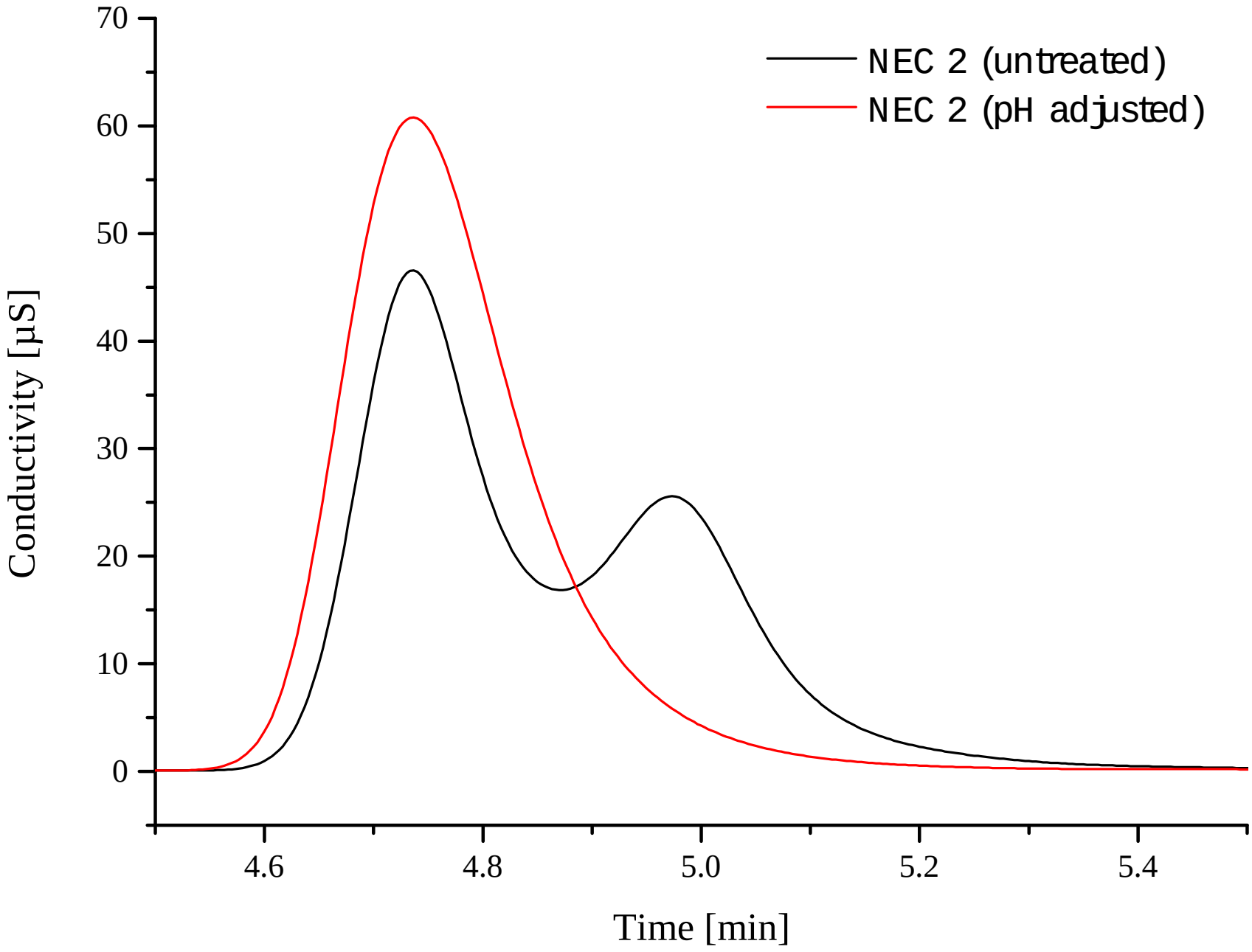
NEC 2 (untreated)
NEC 2 (pH adjusted)
Conductivity [µS]
70
60
50
40
30
20
10
0
4.6
4.8
5.0
5.2
5.4
Time [min]

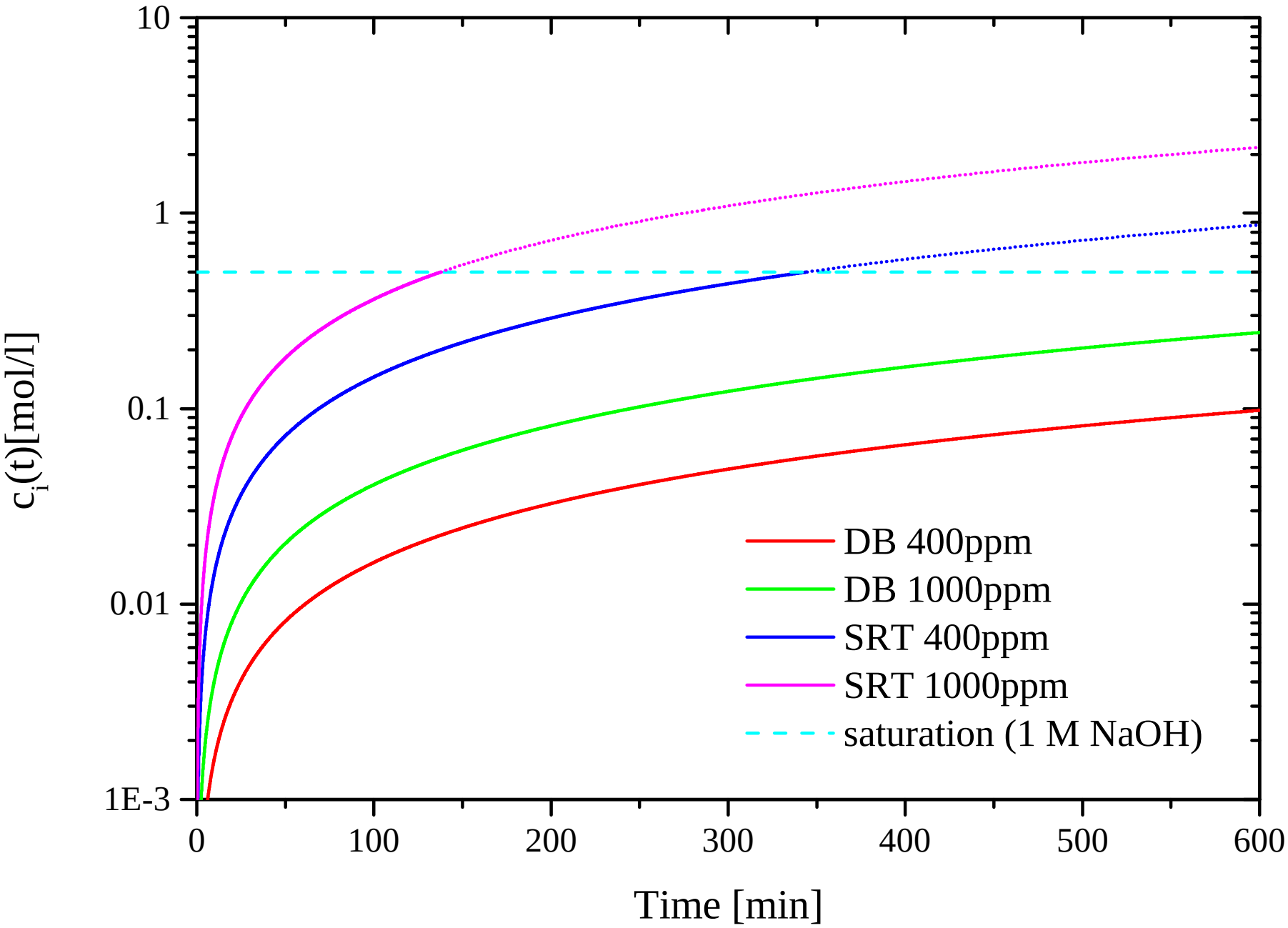
10
1
0.1
0.01
1E-3
0
100
200
300
400
500
600
$c_i(t)$[mol/l]
Time [min]
DB 400ppm
DB 1000ppm
SRT 400ppm
SRT 1000ppm
saturation (1 M NaOH)

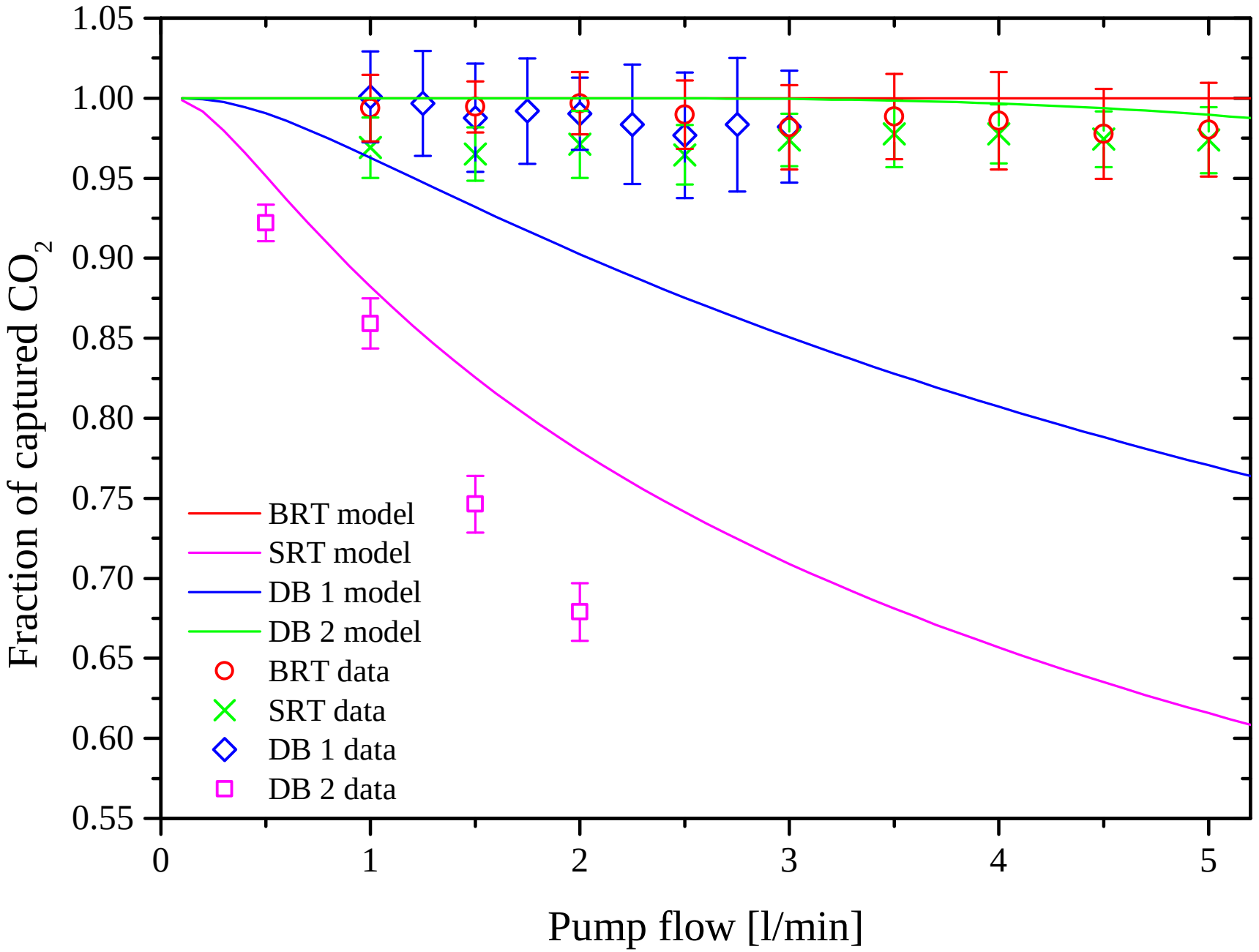
1.05
1.00
0.95
0.90
0.85
0.80
0.75
0.70
0.65
0.60
0.55
0
1
2
3
4
5
Fraction of captured CO_2
Pump flow [l/min]
BRT model
SRT model
DB 1 model
DB 2 model
BRT data
SRT data
DB 1 data
DB 2 data

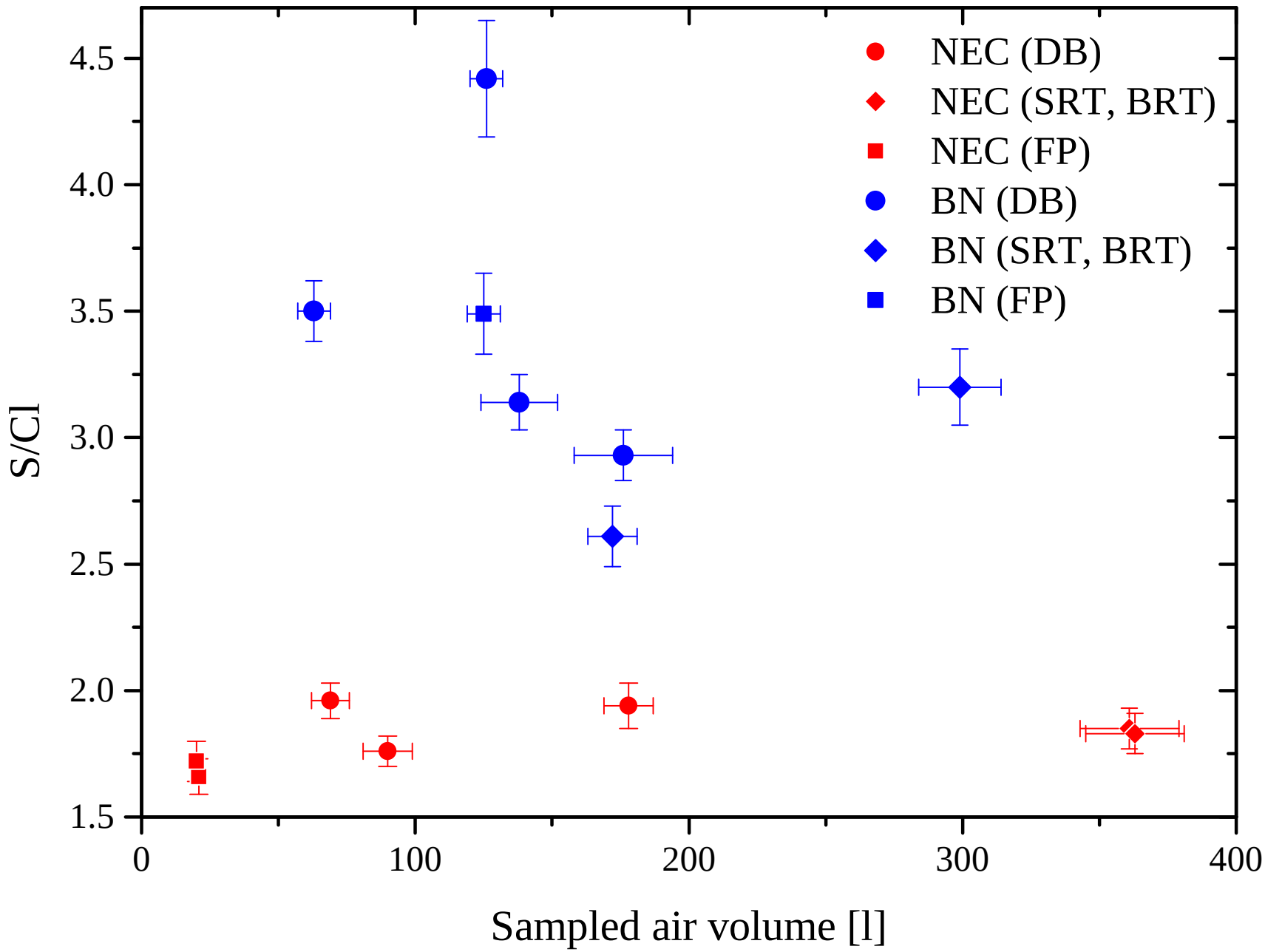
NEC (DB)
NEC (SRT, BRT)
NEC (FP)
BN (DB)
BN (SRT, BRT)
BN (FP)
S/Cl
4.5
4.0
3.5
3.0
2.5
2.0
1.5
0
100
200
300
400
Sampled air volume [l]

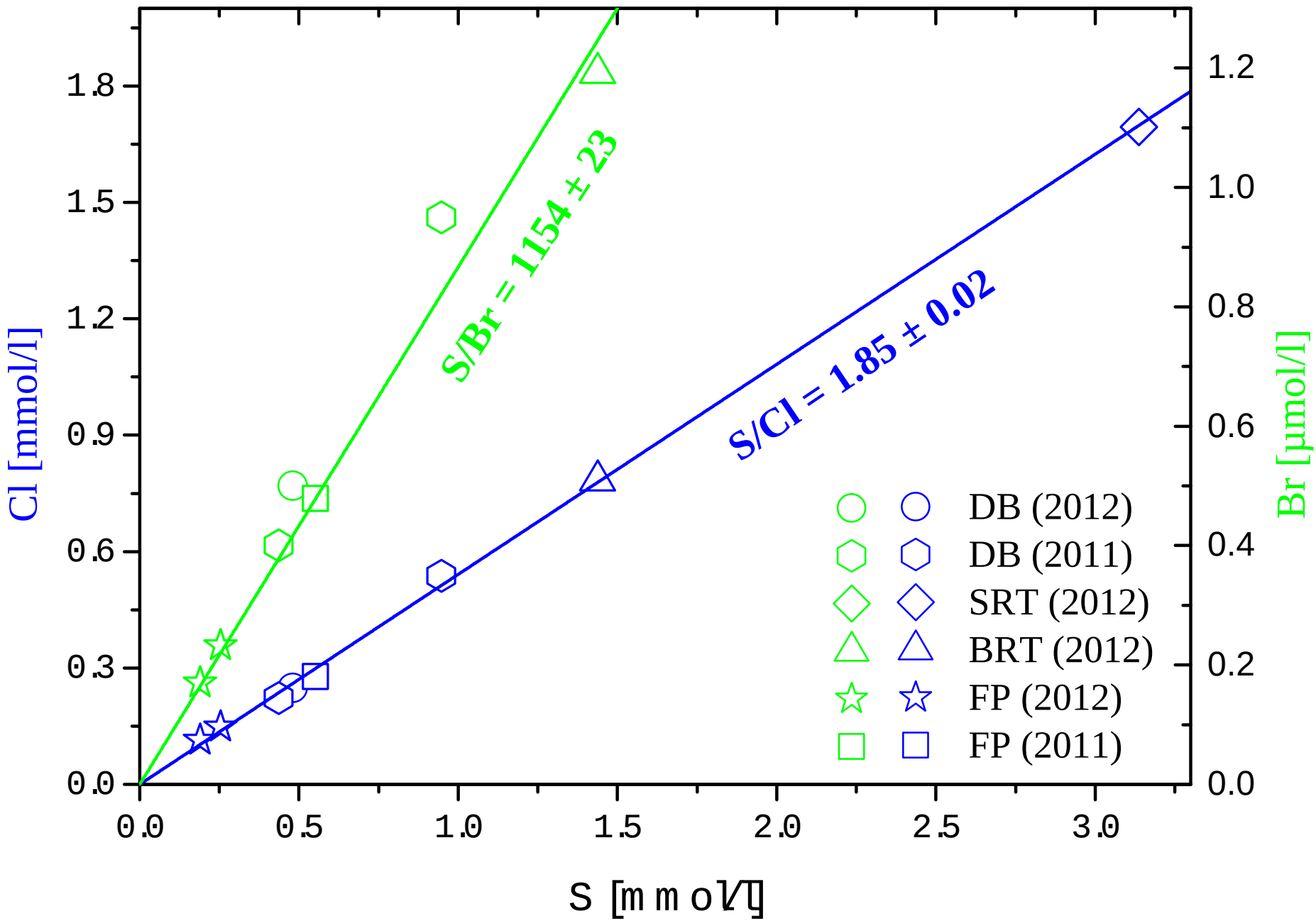
Cl [mmol/l]
Br [µmol/l]
S [mmol/l]
0.0
0.3
0.6
0.9
1.2
1.5
1.8
0.0
0.2
0.4
0.6
0.8
1.0
1.2
0.0
0.5
1.0
1.5
2.0
2.5
3.0
S/Br = 1154 ± 23
S/Cl = 1.85 ± 0.02
DB (2012)
DB (2011)
SRT (2012)
BRT (2012)
FP (2012)
FP (2011)

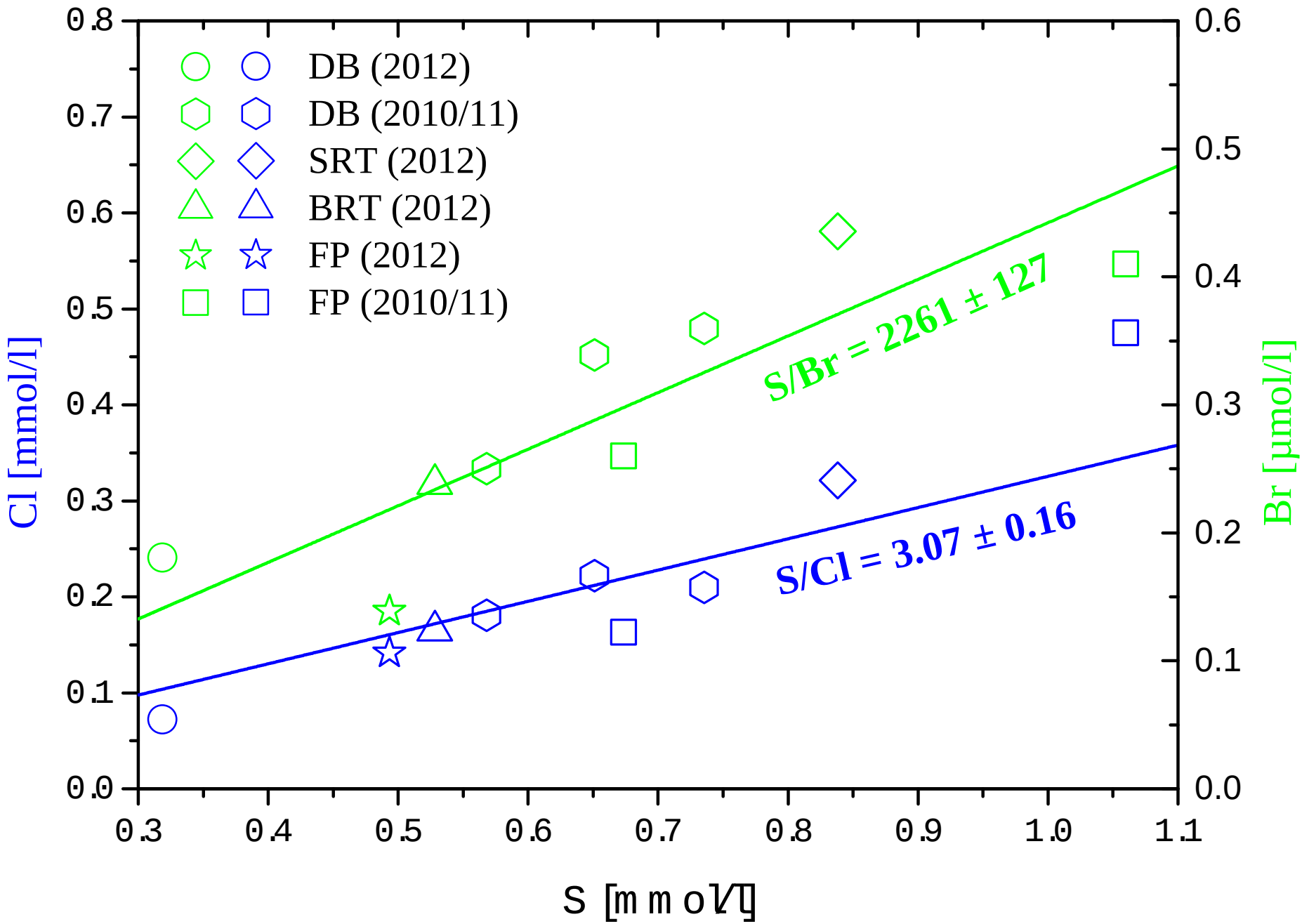
DB (2012)
DB (2010/11)
SRT (2012)
BRT (2012)
FP (2012)
FP (2010/11)
S/Br = 2261 ± 127
S/Cl = 3.07 ± 0.16
Cl [mmol/l]
Br [µmol/l]
S [mmol/l]
0.8
0.7
0.6
0.5
0.4
0.3
0.2
0.1
0.0
0.6
0.5
0.4
0.3
0.2
0.1
0.0
0.3
0.4
0.5
0.6
0.7
0.8
0.9
1.0
1.1

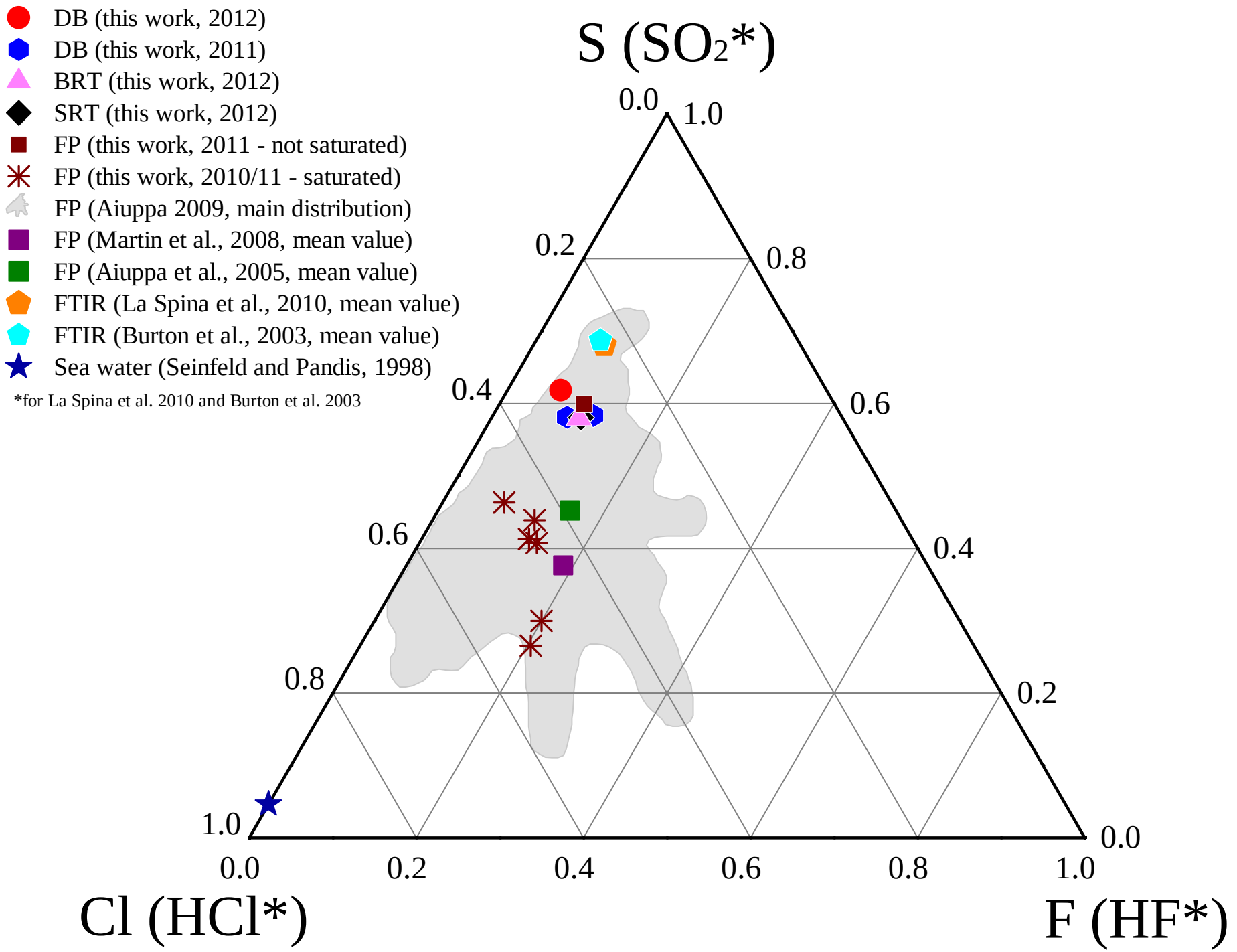
DB (this work, 2012)
DB (this work, 2011)
BRT (this work, 2012)
SRT (this work, 2012)
FP (this work, 2011 - not saturated)
FP (this work, 2010/11 - saturated)
FP (Aiuppa 2009, main distribution)
FP (Martin et al., 2008, mean value)
FP (Aiuppa et al., 2005, mean value)
FTIR (La Spina et al., 2010, mean value)
FTIR (Burton et al., 2003, mean value)
Sea water (Seinfeld and Pandis, 1998)
*for La Spina et al. 2010 and Burton et al. 2003
S (SO2*)
Cl (HCl*)
F (HF*)
0.0
0.2
0.4
0.6
0.8
1.0

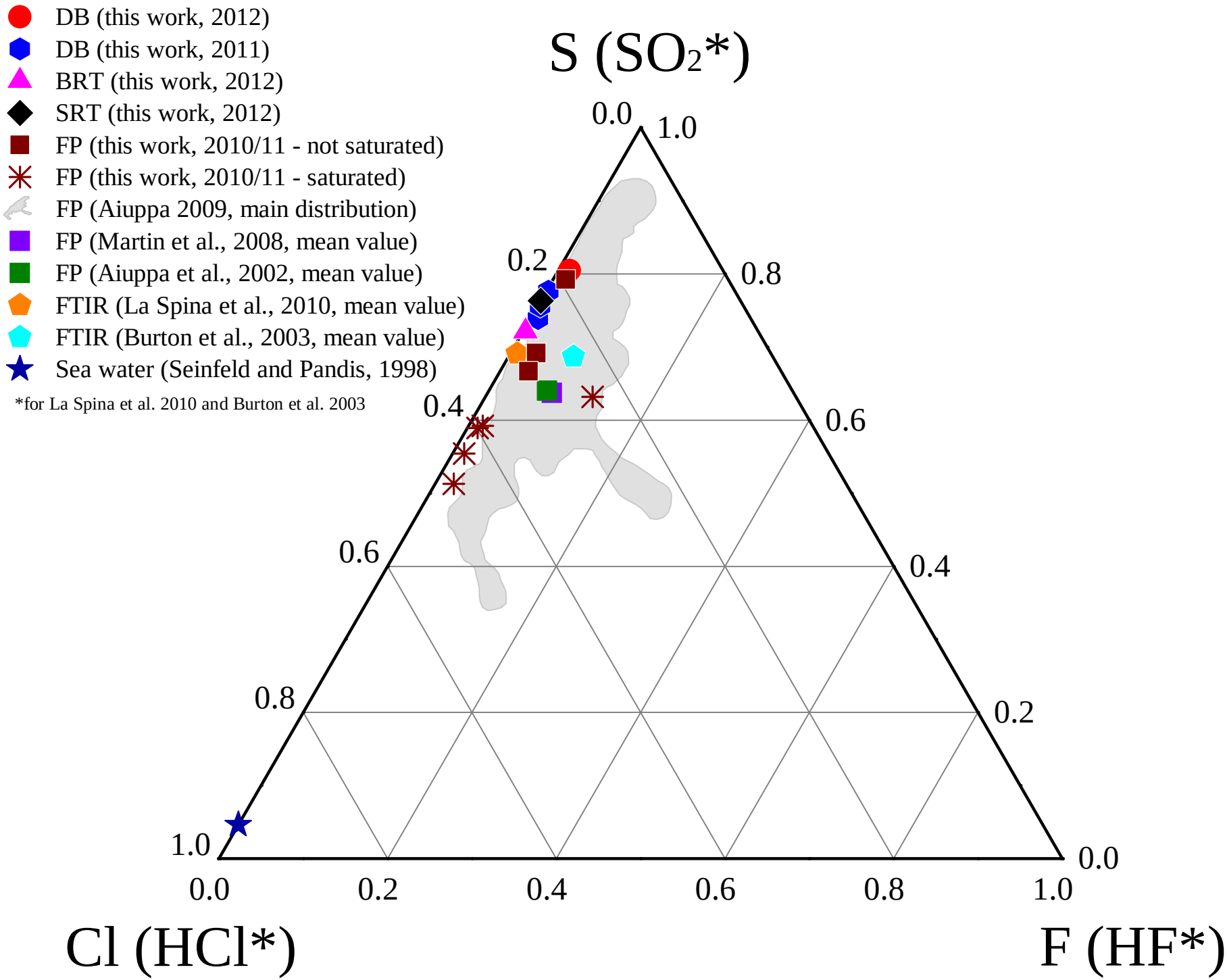
DB (this work, 2012)
DB (this work, 2011)
BRT (this work, 2012)
SRT (this work, 2012)
FP (this work, 2010/11 - not saturated)
FP (this work, 2010/11 - saturated)
FP (Aiuppa 2009, main distribution)
FP (Martin et al., 2008, mean value)
FP (Aiuppa et al., 2002, mean value)
FTIR (La Spina et al., 2010, mean value)
FTIR (Burton et al., 2003, mean value)
Sea water (Seinfeld and Pandis, 1998)
*for La Spina et al. 2010 and Burton et al. 2003
S (SO2*)
Cl (HCl*)
F (HF*)
0.0
0.2
0.4
0.6
0.8
1.0

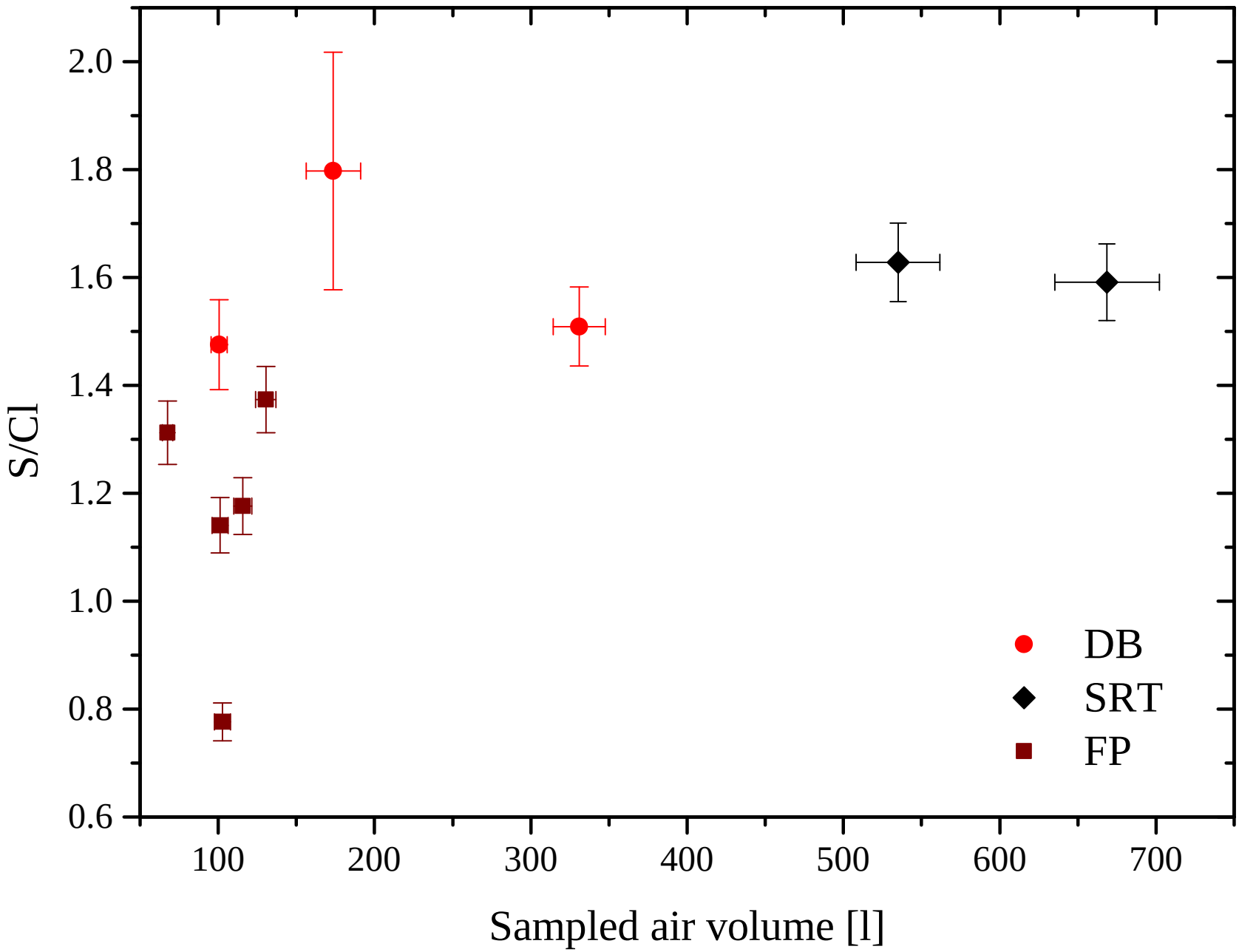
S/Cl
2.0
1.8
1.6
1.4
1.2
1.0
0.8
0.6
100
200
300
400
500
600
700
Sampled air volume [l]
DB
SRT
FP

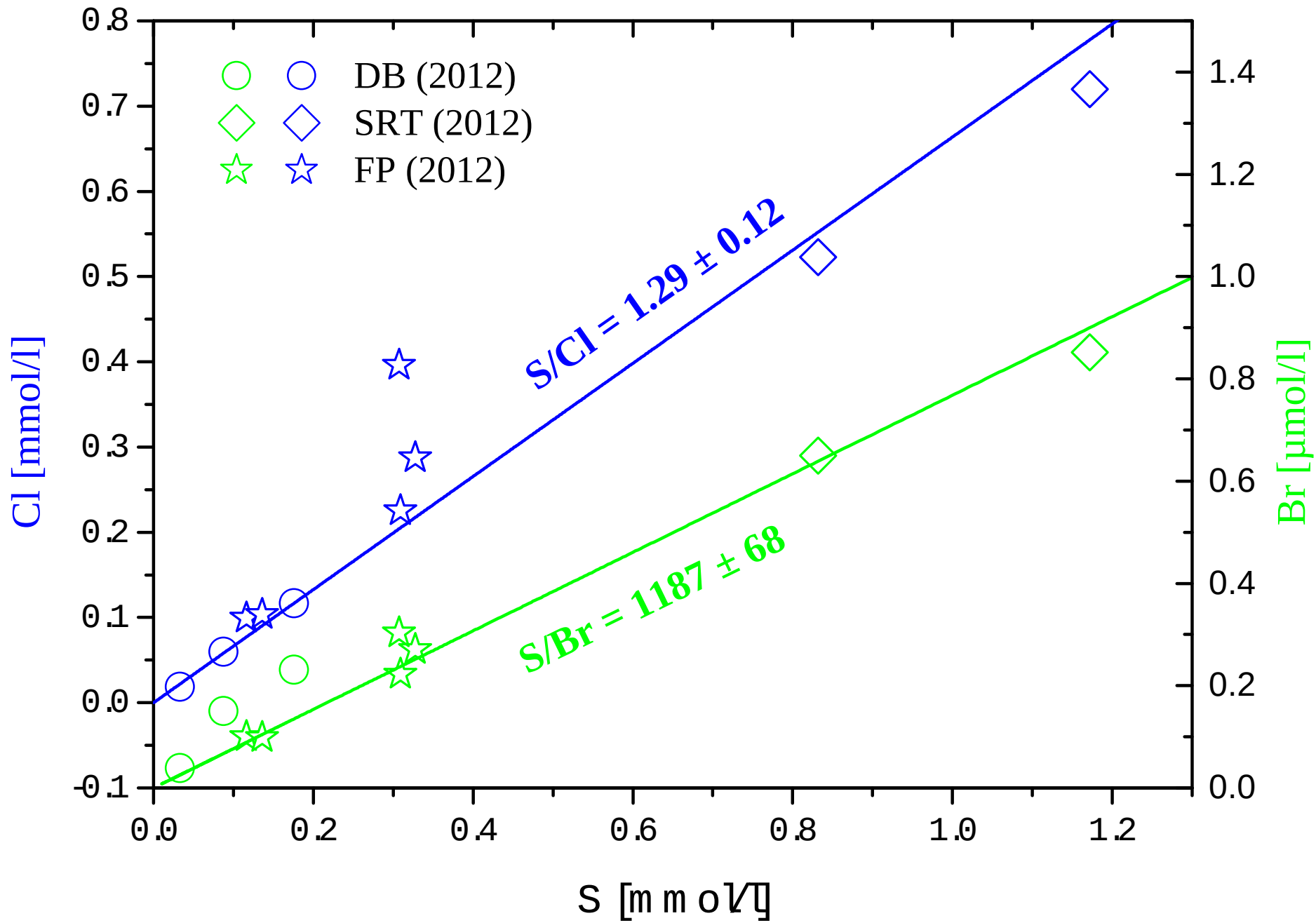
DB (2012)
SRT (2012)
FP (2012)
S/Cl = 1.29 ± 0.12
S/Br = 1187 ± 68
Cl [mmol/l]
Br [µmol/l]
S [mmol/l]
0.8
0.7
0.6
0.5
0.4
0.3
0.2
0.1
0.0
-0.1
1.4
1.2
1.0
0.8
0.6
0.4
0.2
0.0
0.0
0.2
0.4
0.6
0.8
1.0
1.2

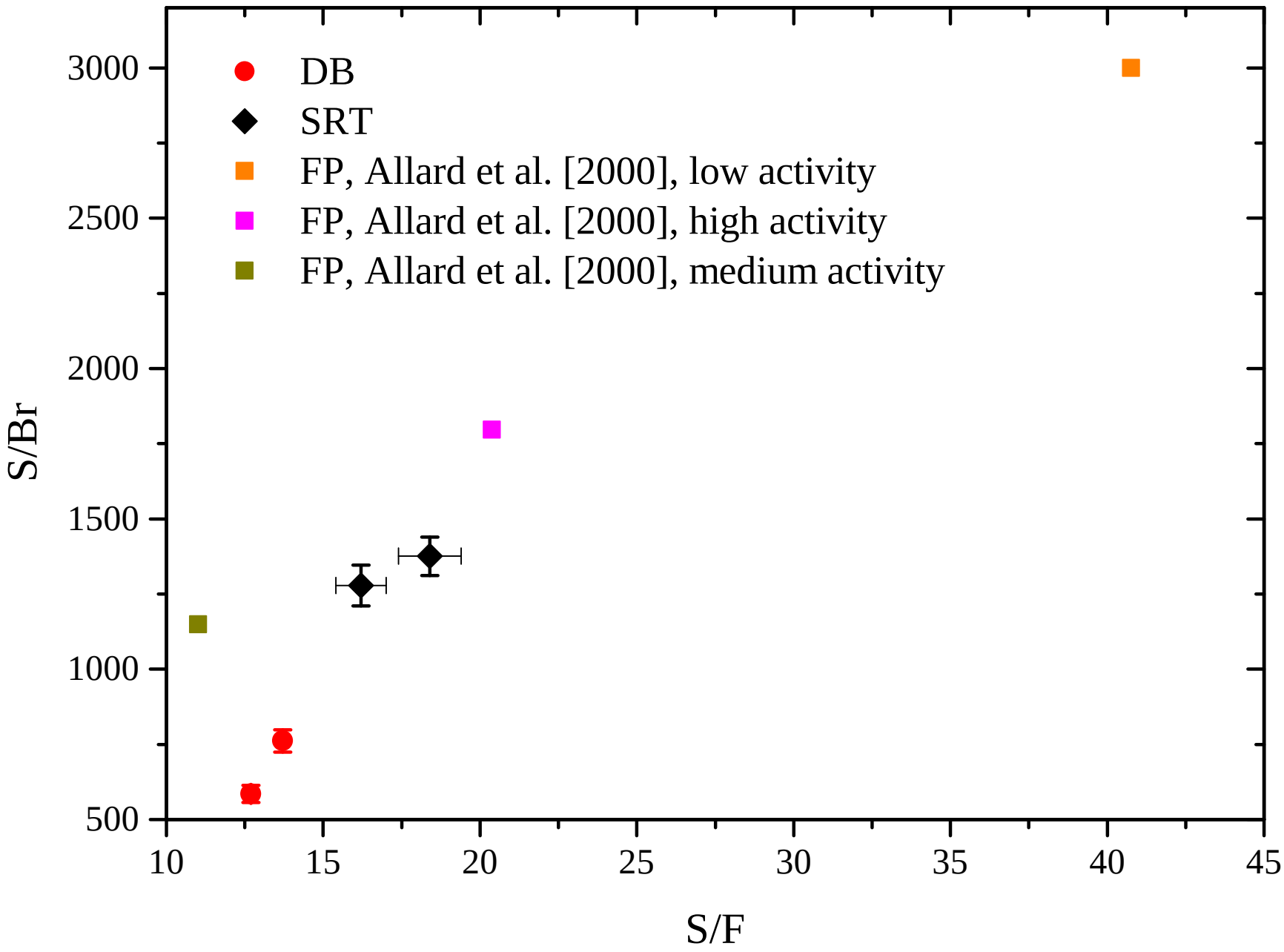
DB
SRT
FP, Allard et al. [2000], low activity
FP, Allard et al. [2000], high activity
FP, Allard et al. [2000], medium activity
S/Br
S/F
3000
2500
2000
1500
1000
500
10
15
20
25
30
35
40
45

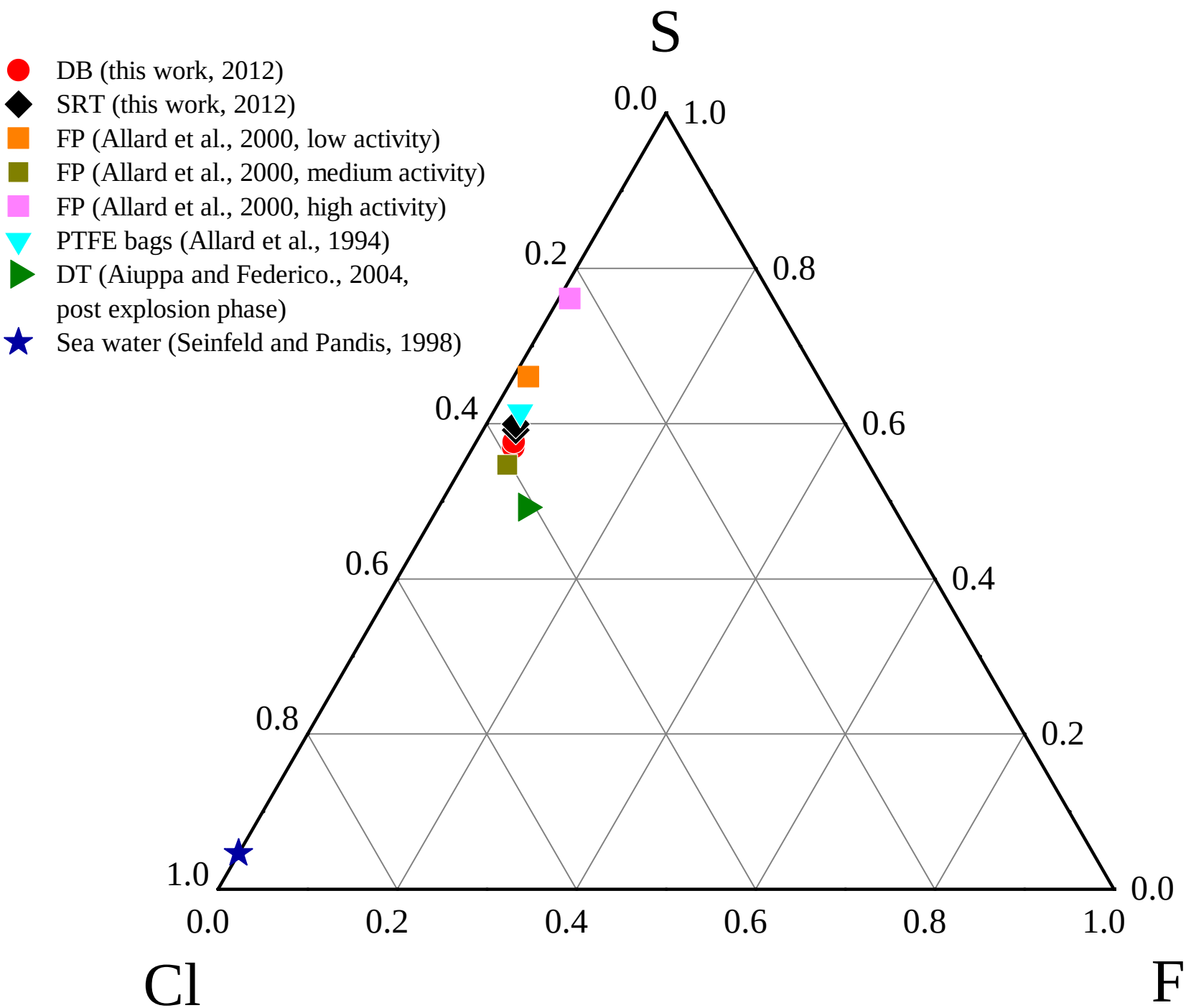
DB (this work, 2012)
SRT (this work, 2012)
FP (Allard et al., 2000, low activity)
FP (Allard et al., 2000, medium activity)
FP (Allard et al., 2000, high activity)
PTFE bags (Allard et al., 1994)
DT (Aiuppa and Federico., 2004, post explosion phase)
Sea water (Seinfeld and Pandis, 1998)
S
0.0
1.0
0.2
0.8
0.4
0.6
0.6
0.4
0.8
0.2
1.0
0.0
0.0
0.2
0.4
0.6
0.8
1.0
Cl
F

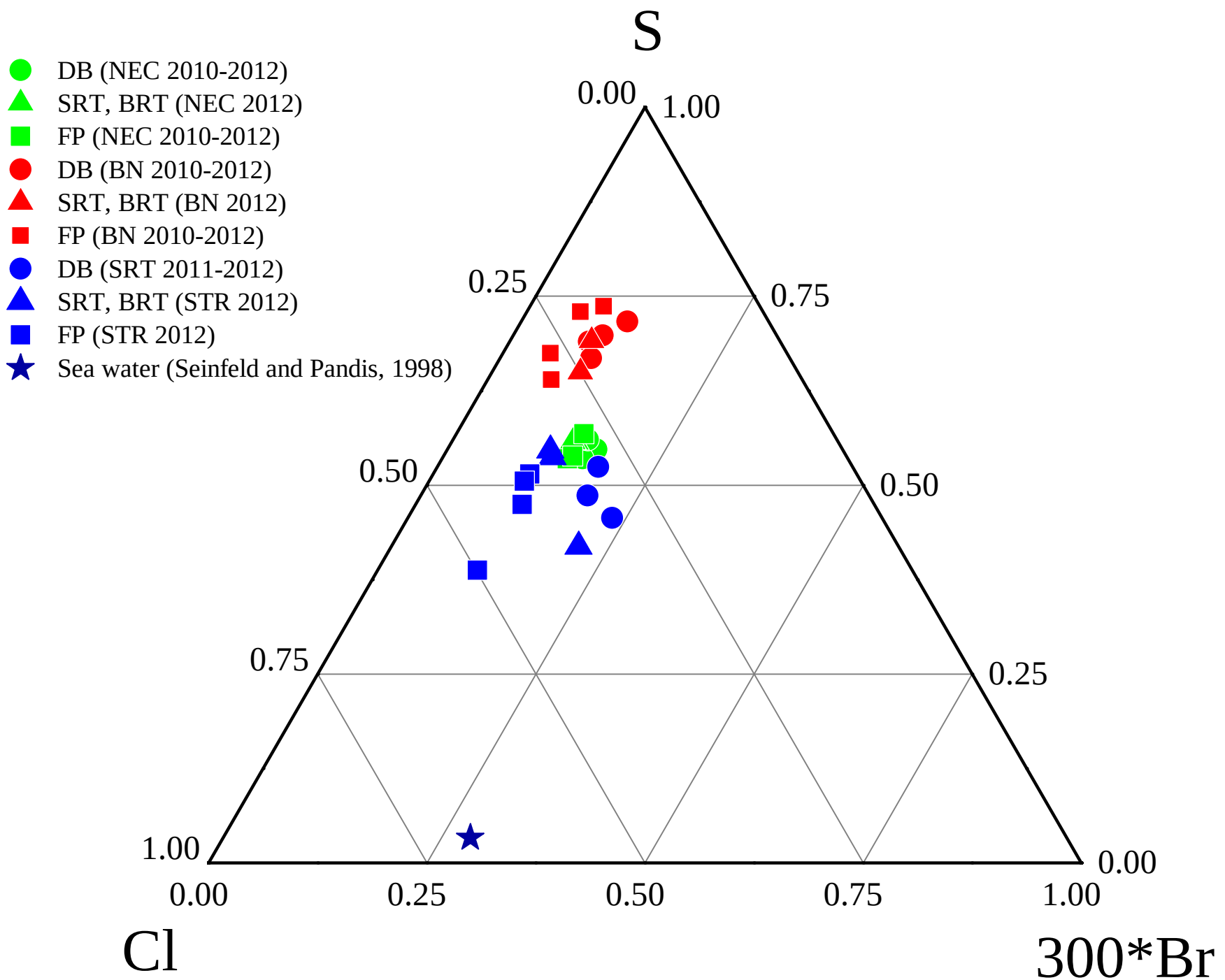
DB (NEC 2010-2012)
SRT, BRT (NEC 2012)
FP (NEC 2010-2012)
DB (BN 2010-2012)
SRT, BRT (BN 2012)
FP (BN 2010-2012)
DB (SRT 2011-2012)
SRT, BRT (STR 2012)
FP (STR 2012)
Sea water (Seinfeld and Pandis, 1998)
S
0.00
1.00
0.25
0.75
0.50
0.50
0.75
0.25
1.00
0.00
0.00
0.25
0.50
0.75
1.00
Cl
300*Br